COMPMECH
Computational Mechanics & Advanced Materials

UNIVERSITÀ DI PAVIA

Dottorato di Ricerca in
Tecnologie per la Salute, Bioingegneria e Bioinformatica
XXXIII ciclo

Carotid artery and stenting: from geometrical analysis to computational hemodynamics

Giovanni Maria Formato

Tutor
Michele Conti

Pavia, 23/02/2021

AIM OF THE THESIS

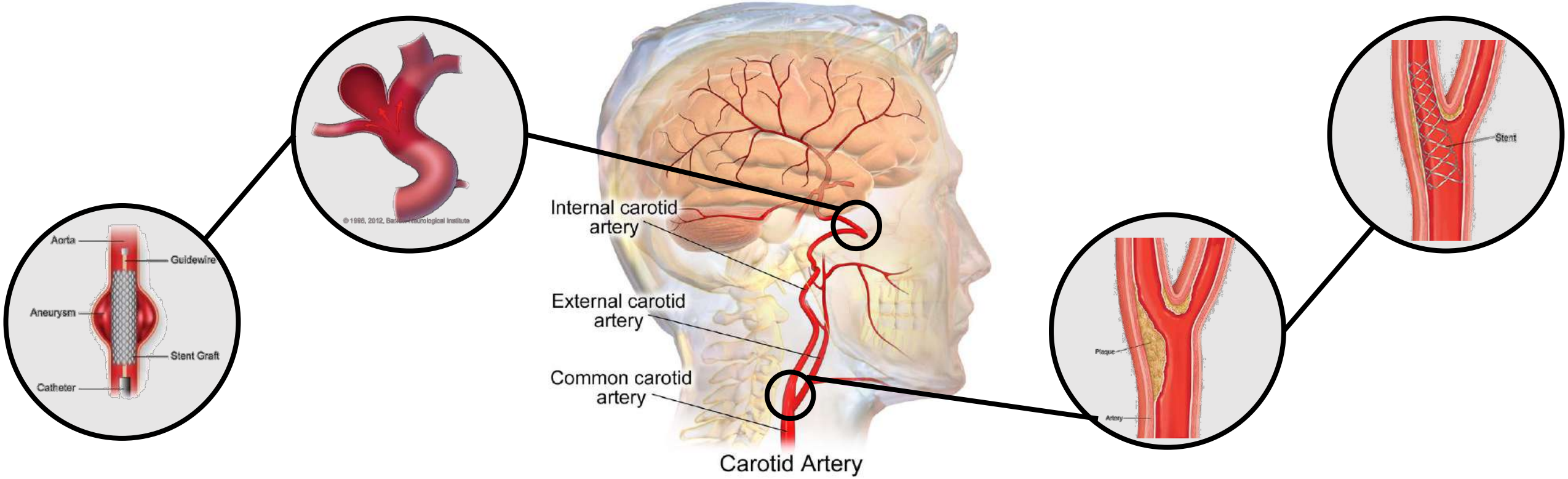

I. Set-up innovative computational tools for **geometrical** and **hemodynamic** analysis in the carotid artery

II. Apply the developed tools in different clinical perspectives of **arteriosclerosis**

MULTIFACTORIALITY OF ARTERIOSCLEROSIS

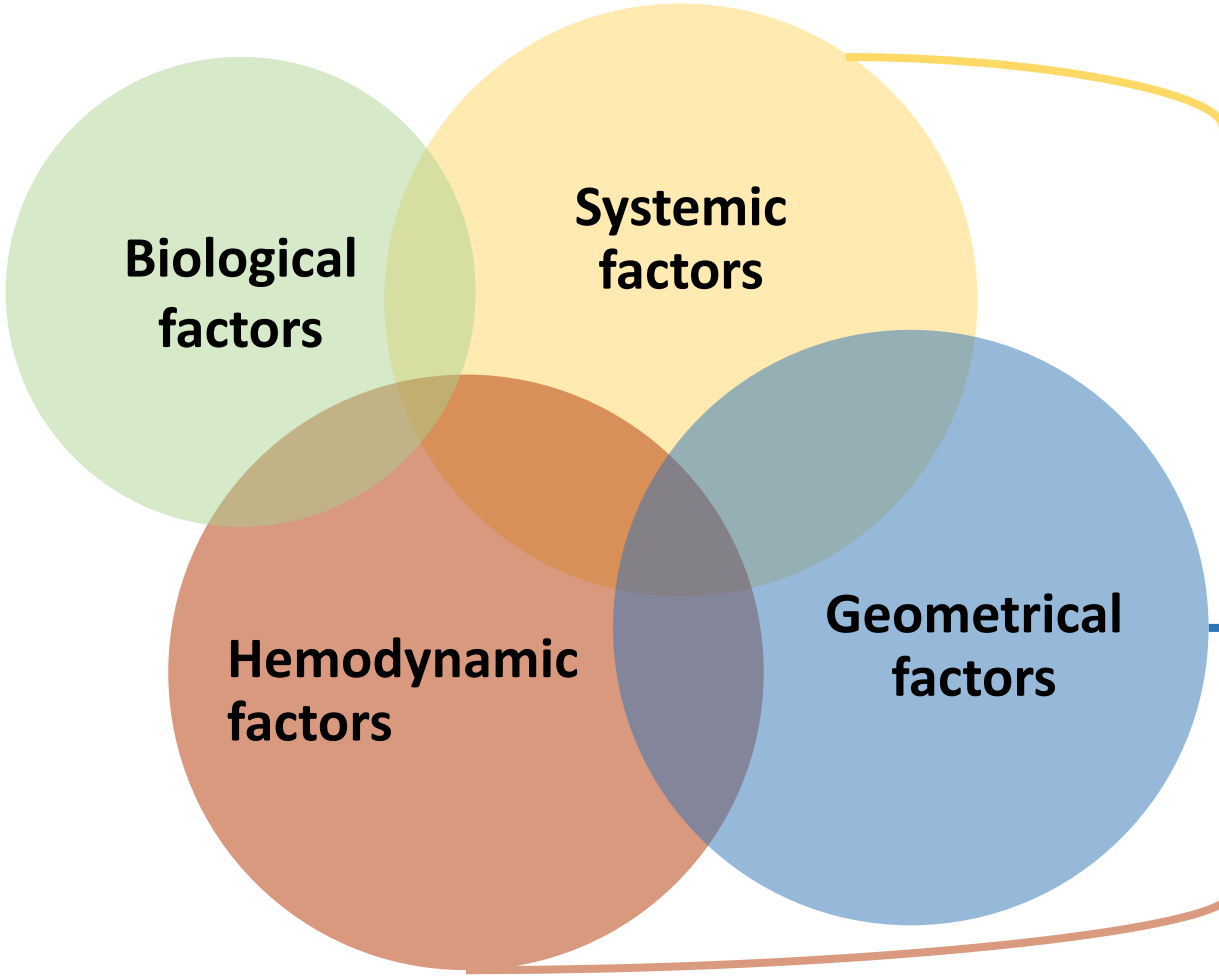

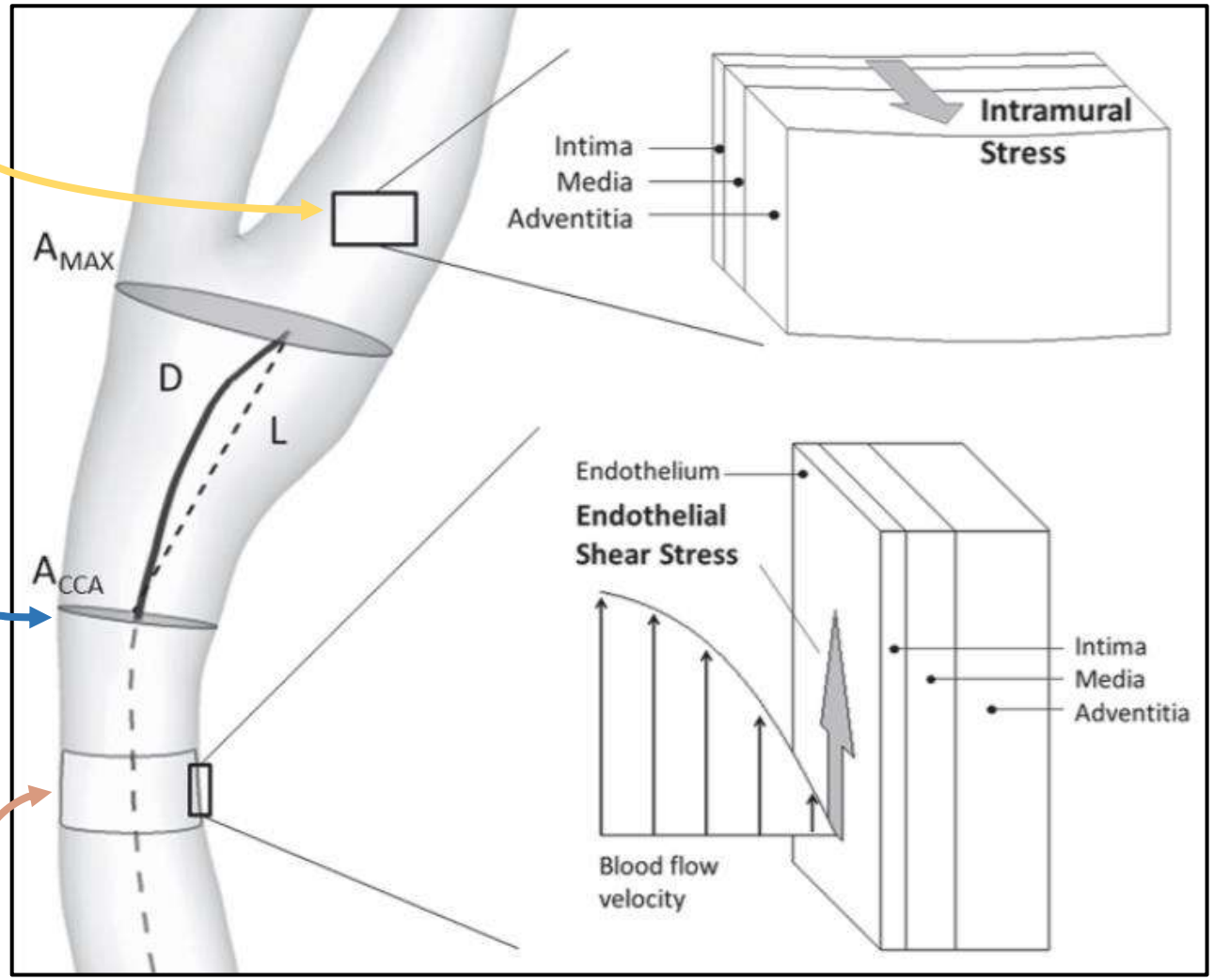

Susic et al. 1997
Han et al. 2012

Morbiducci et al. 2016

THESIS OUTLINE

I. Arterial morphometry, cerebral perfusion and hypertension

- **Method:** Framework for automatic splitting and morphometric analysis of carotid and vertebral arteries
- **Application:** Analysis of vascular morhometry and blood flow in a multipatient dataset of 112 normotensive/hypertensives

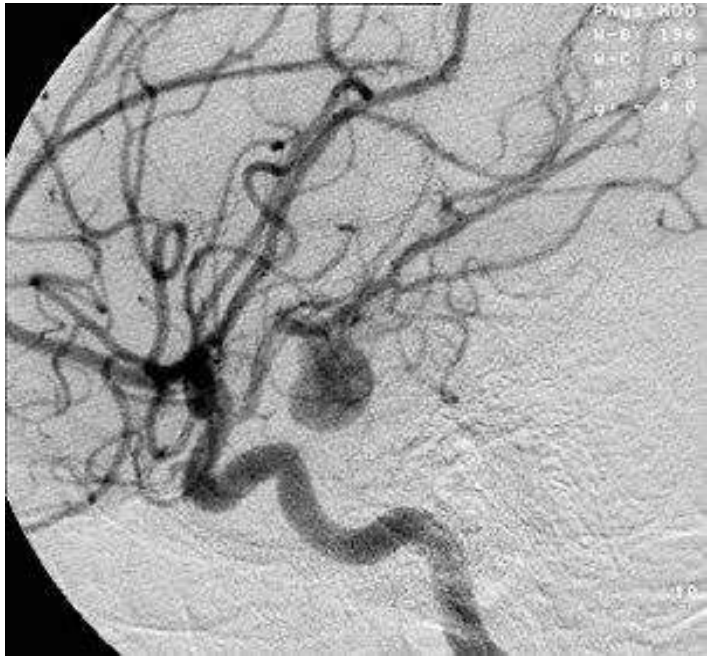

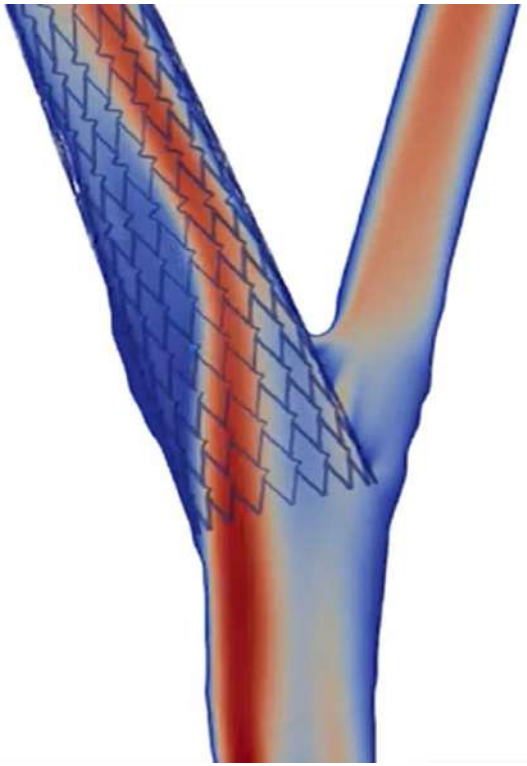

II. Carotid stenting, hemodynamics and restenosis

- **Method:** Framework for analysis of post-stenting carotid hemodynamics exploiting the immersed approach
- **Application:** Proof-of-concept study assessing the impact of 4 stent designs on carotid hemodynamics

Arterial morphometry, cerebral perfusion and hypertension

UNIVERSITÀ DI PAVIA

University of BRISTOL

BACKGROUND AND AIM OF THE STUDY

- Cushing mechanism: insufficient cerebral flow & hypertension *(Paton et al. 2009)*
- Prevalence in hypertensives of congenital variants of vertebral arteries *(Warnert et al. 2016)*
- Insufficient data concerning carotid arteries *(Pancera et al. 2000)*

- **Global measures**
- **Manual measures**

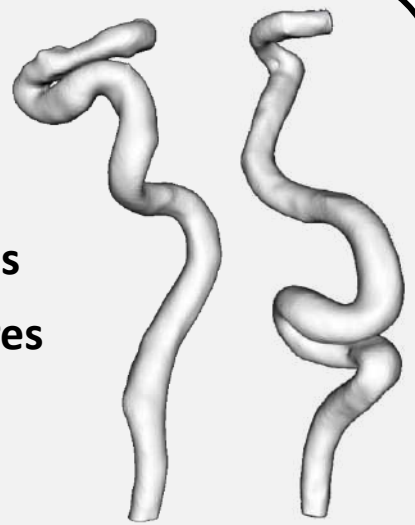

Study on a population of **112 participants** if hypertensives exhibit specific morphometric features of carotid and vertebral vessels

Framework to automatically:

→ Split vessels
→ Extract morphometric features of local tracts

FRAMEWORK FOR VASCULAR SPLITTING

MEDICAL IMAGE SEGMENTATION → **CENTERLINE** → **CURVATURE ANALYSIS** → **CAROTID SPLITTING**

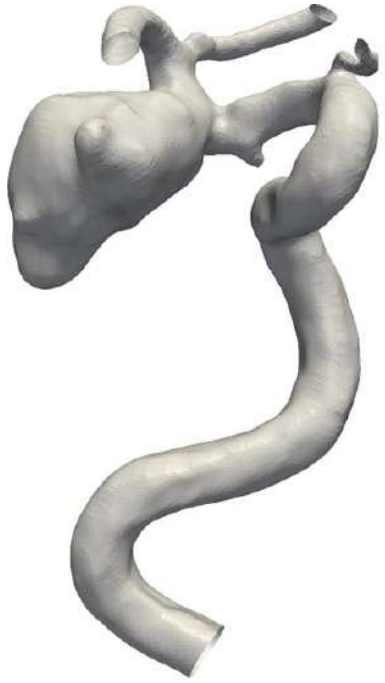

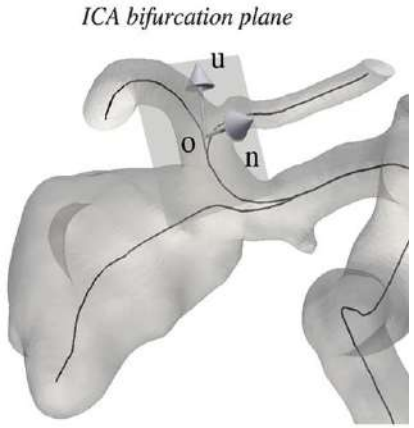

Accurate curvature computation

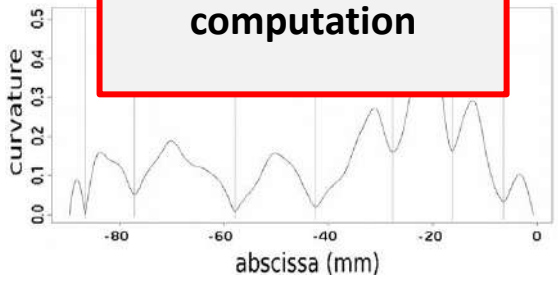

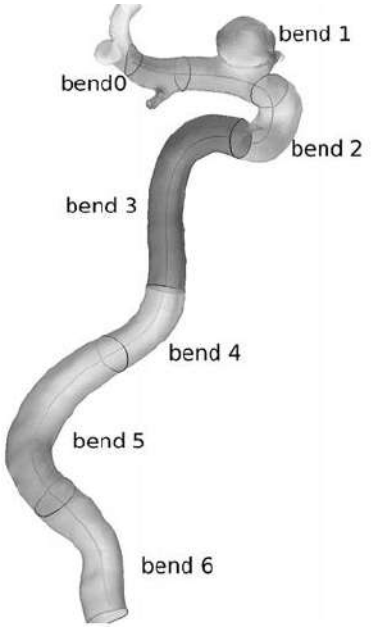

Piccinelli et al. 2011

CURVATURE COMPUTATION BY CENTRAL DIFFERENCE

STL 3D MODEL

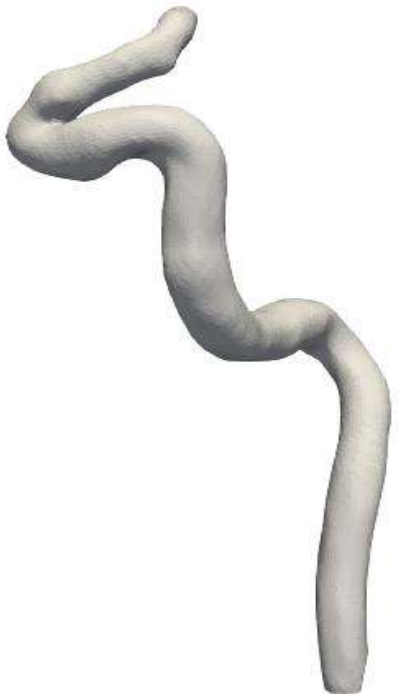

CENTERLINE

Resampling=1 mm
(≈100 points)

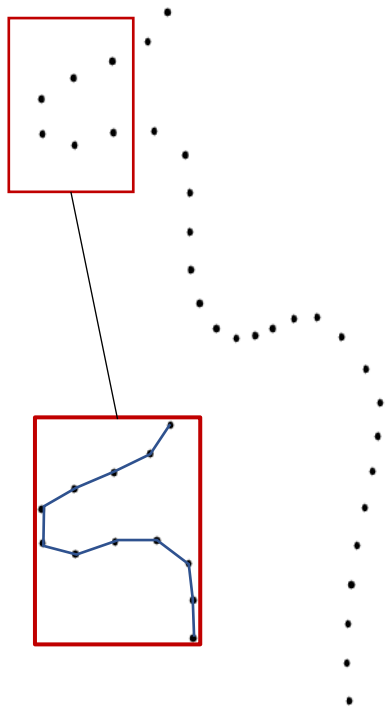

CENTERLINE COMPONENTS

$$c(s) = (x(s), y(s), z(s))$$

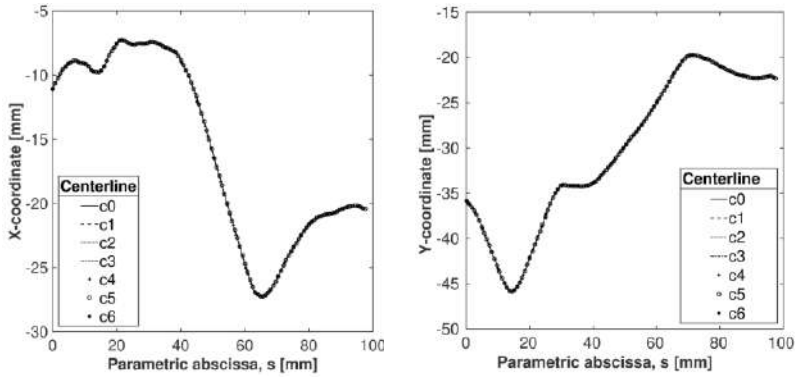

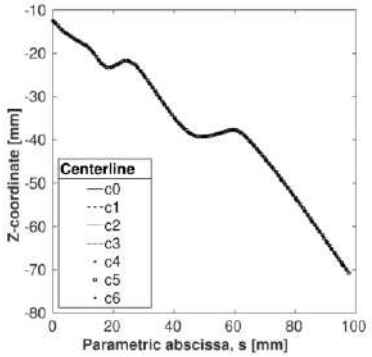

CURVATURE

$$curv_c(s) = \frac{\| c'(s) \times c''(s) \|}{\| c'(s) \|^3}$$

CENTRAL DIFFERENCE

INACCURATE

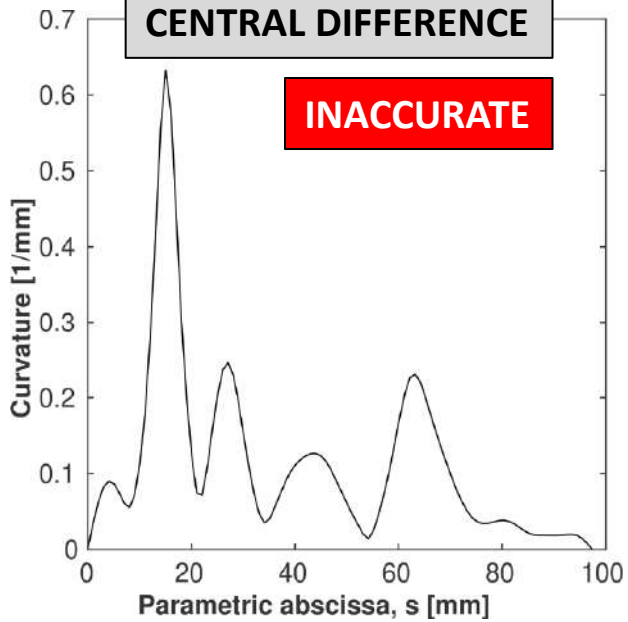

SPATIALLY ADAPTIVE FREE KNOT REGRESSION SPLINES

SARS: Spatially Adaptive free-knot Regression Splines

FIT EACH COMPONENT WITH ANALYTICAL FUNCTION

EXACT DERIVATION

ANALYTICAL CURVATURE

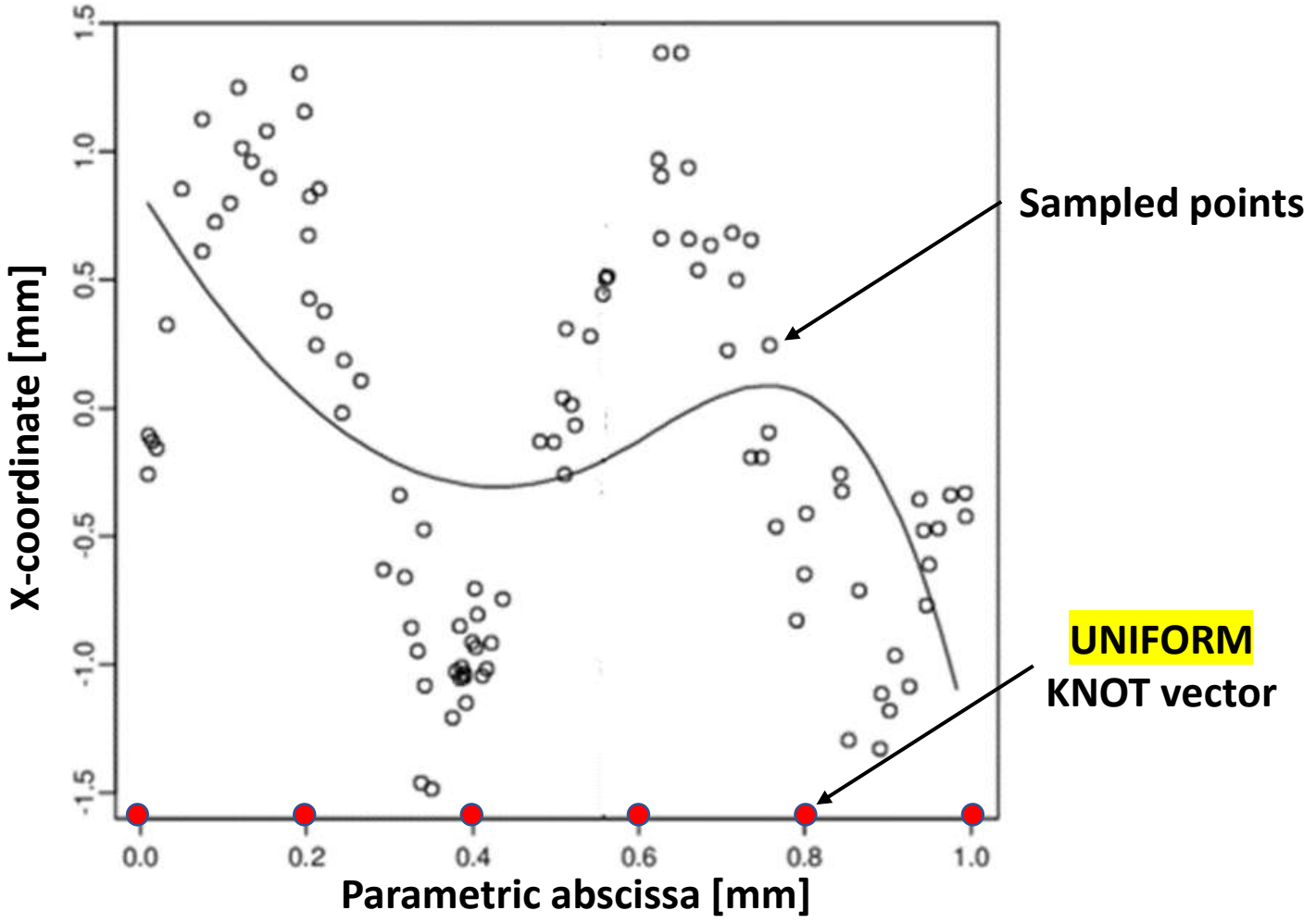

Sangalli et al. 2009
Zhou and Shen 2001

SPATIALLY ADAPTIVE FREE KNOT REGRESSION SPLINES

SARS: Spatially Adaptive free-knot Regression Splines

FIT EACH COMPONENT
WITH
ANALYTICAL FUNCTION

EXACT DERIVATION

ANALYTICAL CURVATURE

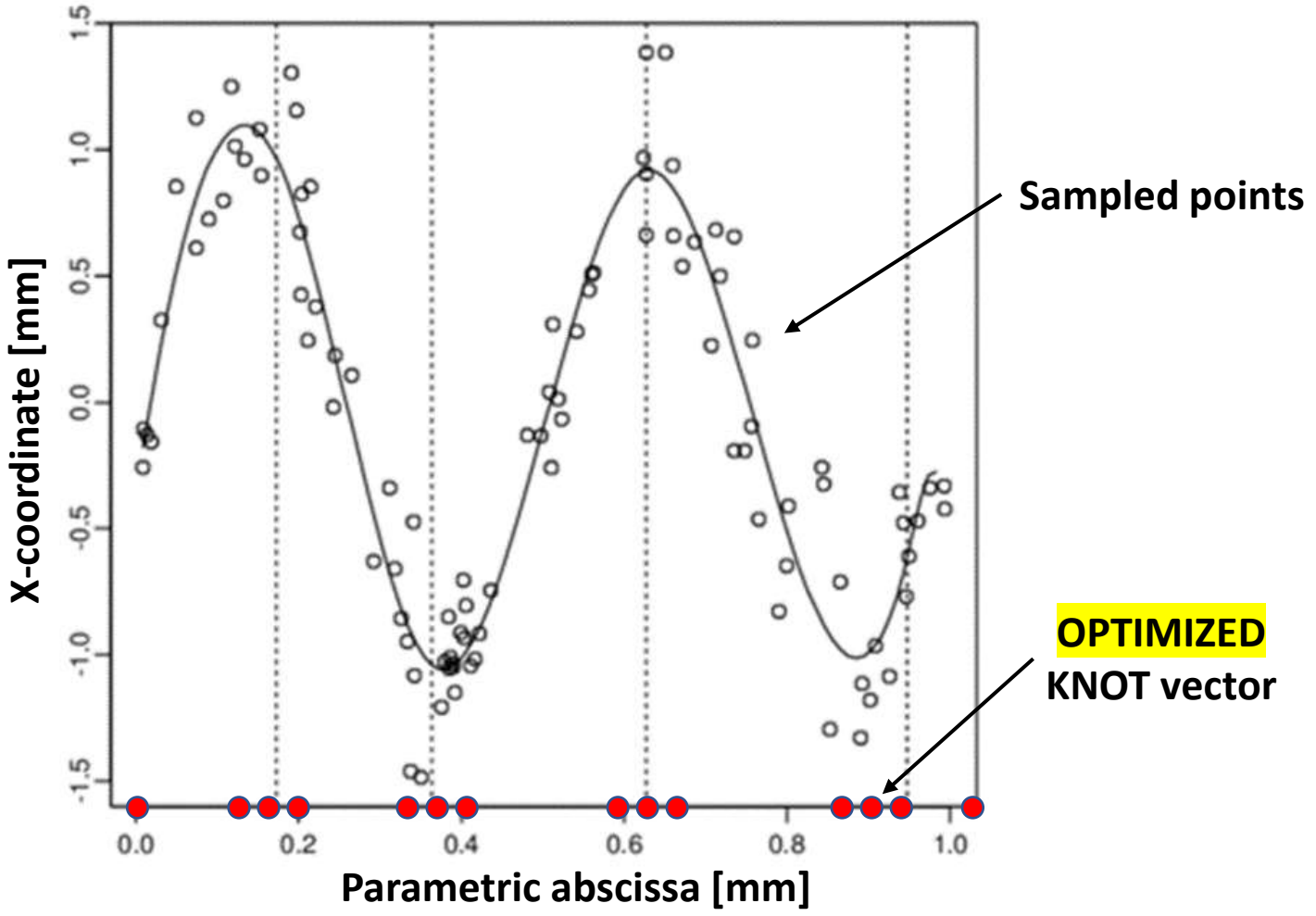

Sangalli et al. 2009
Zhou and Shen 2001

SPATIALLY ADAPTIVE FREE KNOT REGRESSION SPLINES

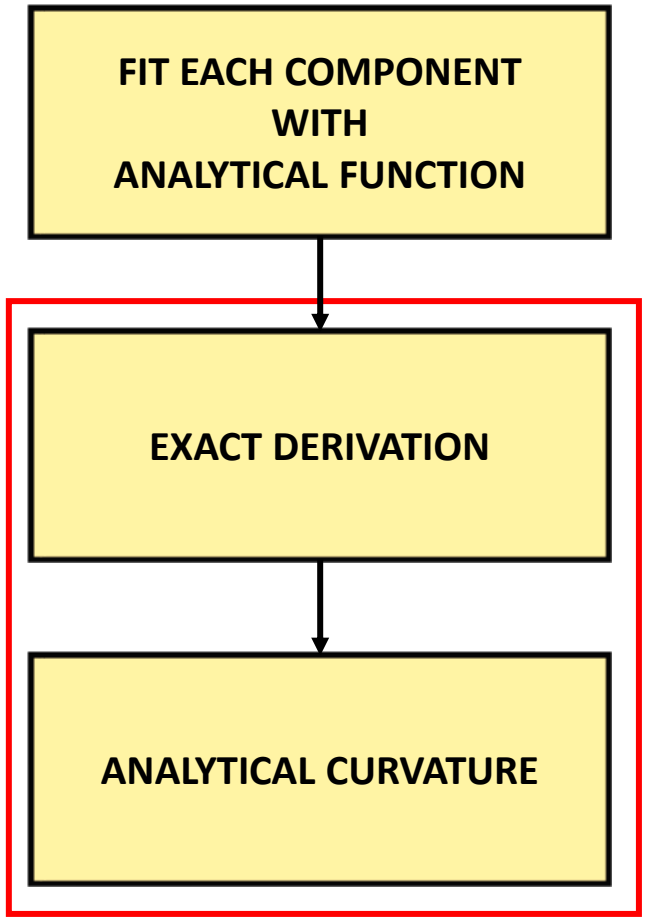

Sangalli et al. 2009
Zhou and Shen 2001

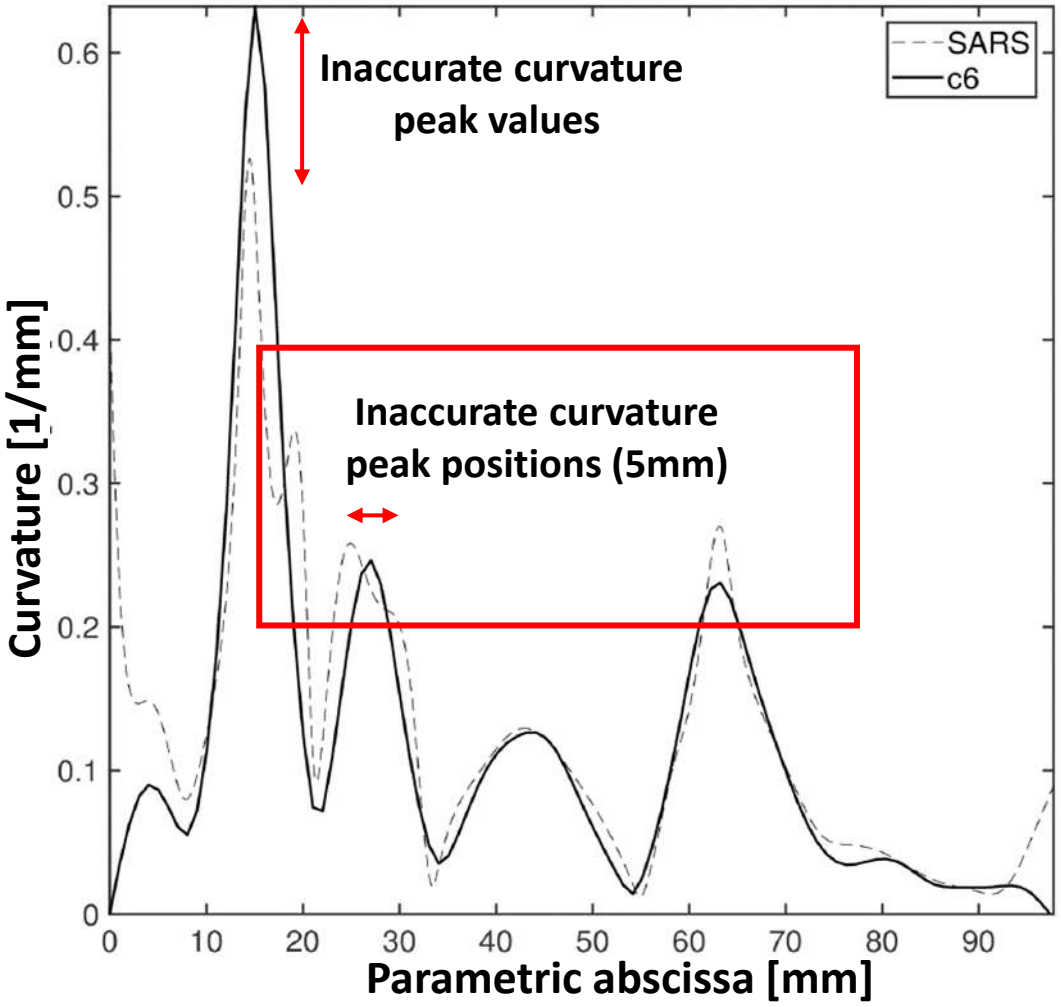

CAROTID SPLITTING

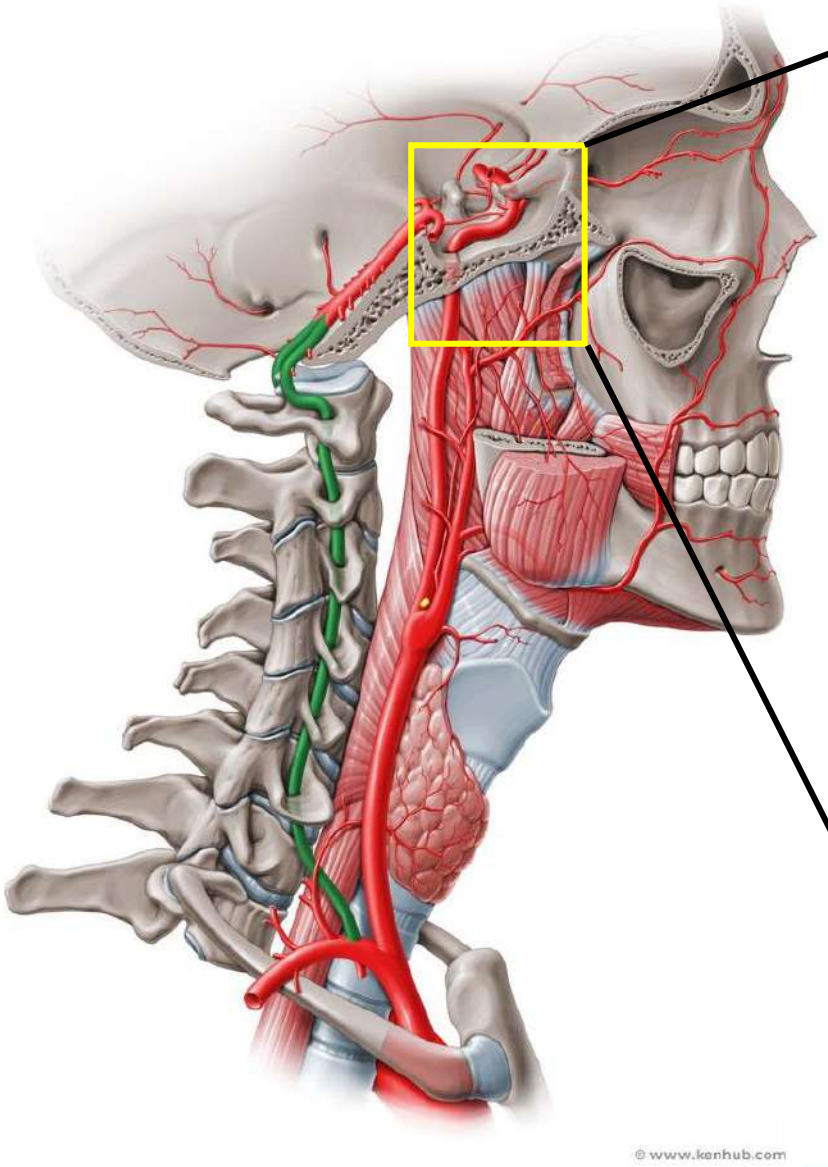

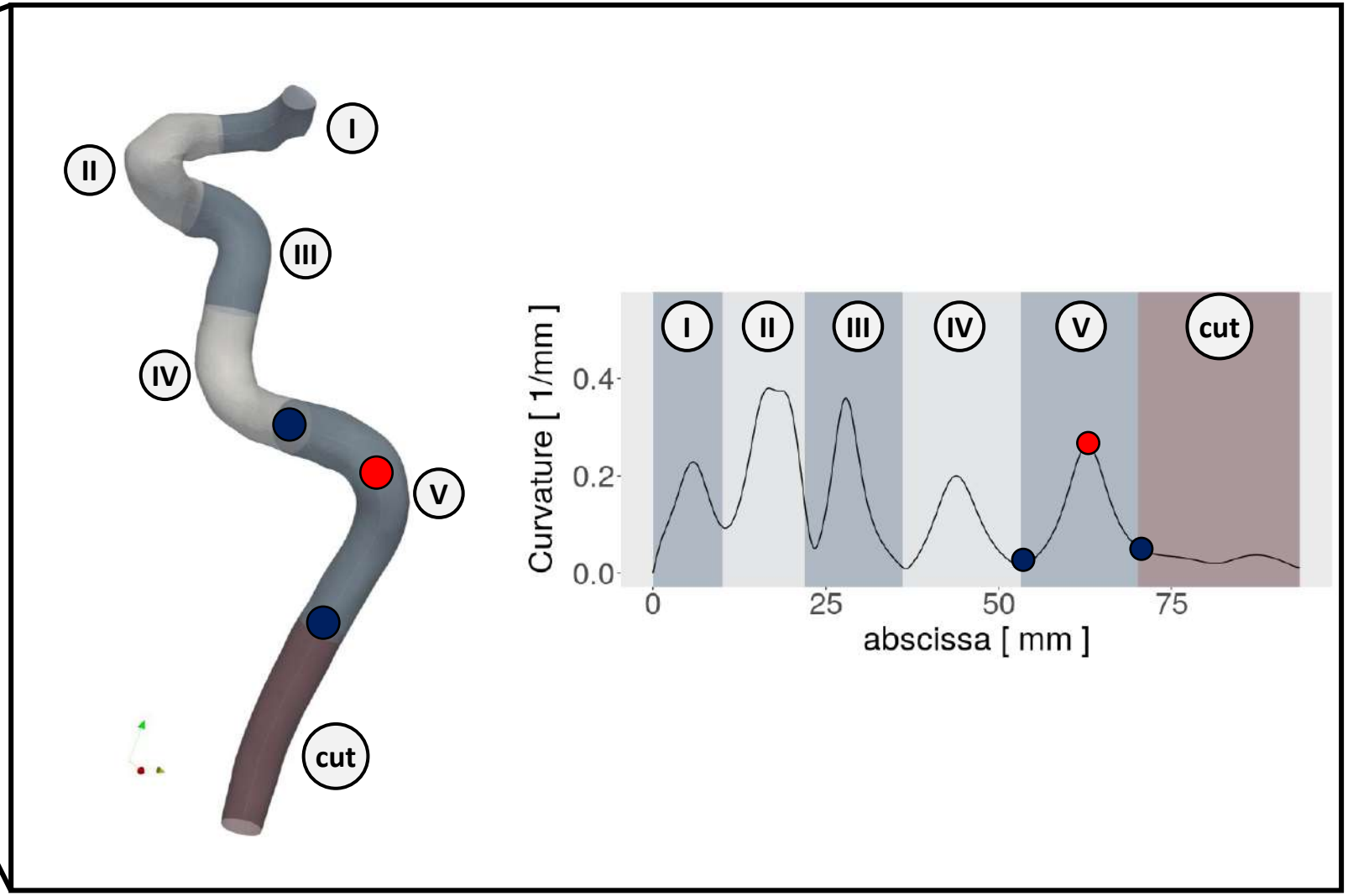

VERTEBRAL SPLITTING

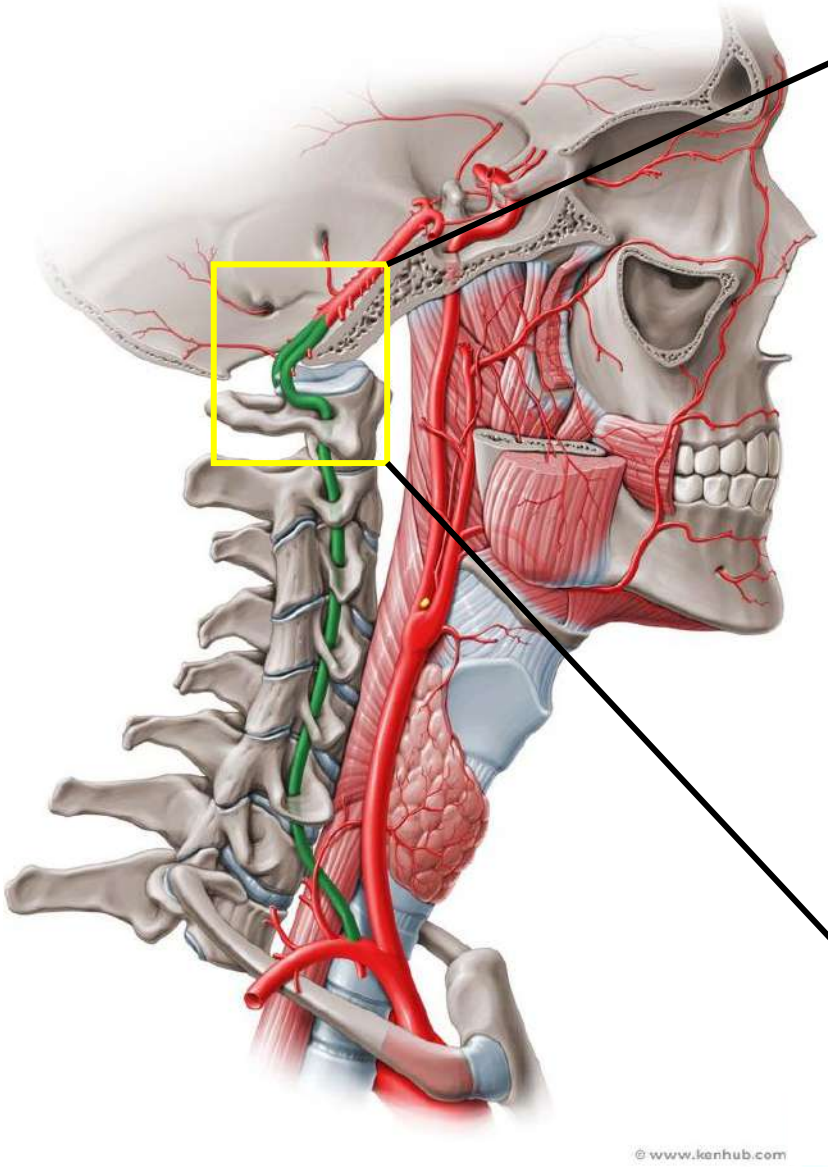

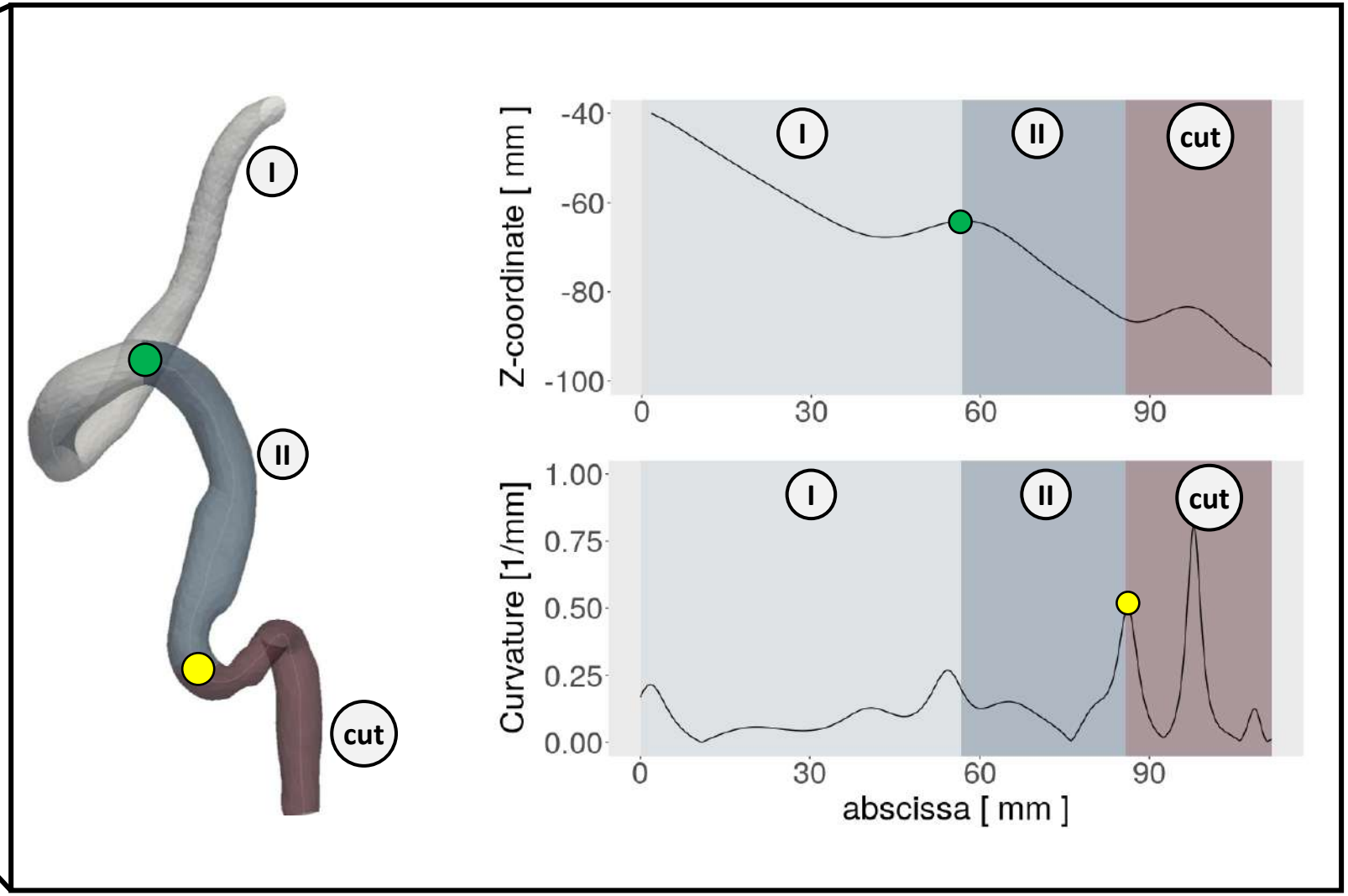

AUTOMATIC MORPHOMETRIC MEASUREMENTS

SPLITTING

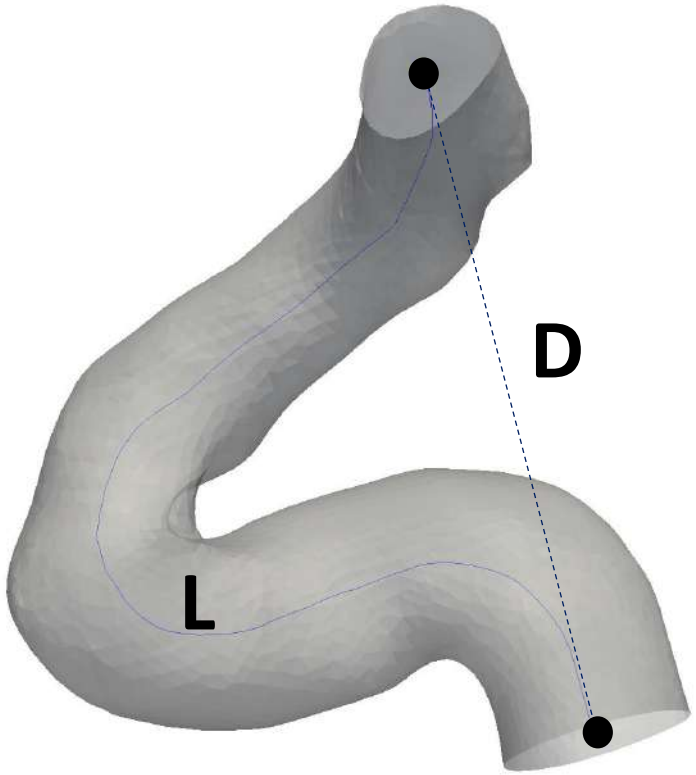

Tortuosity = L/D

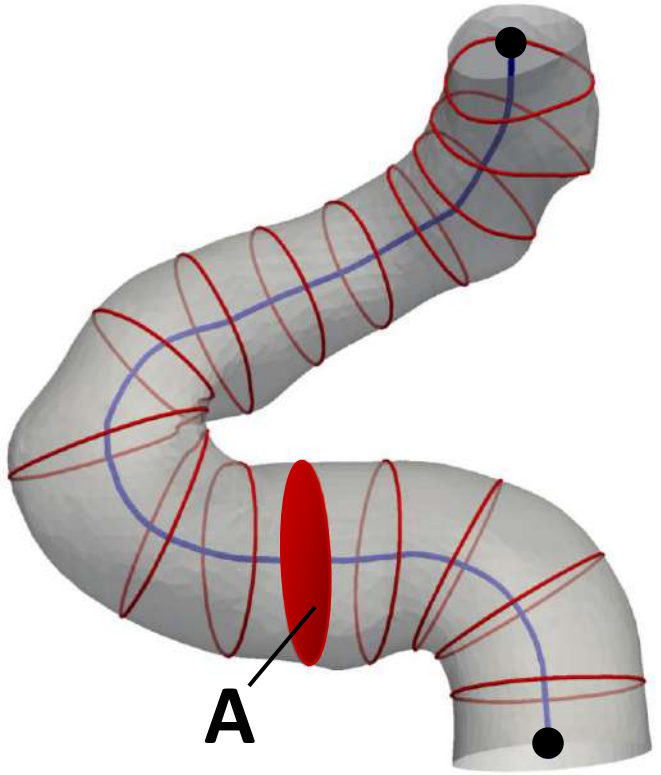

Caliber

MORPHOMETRIC DATA

MORPHOMETRIC ANALYSIS: MULTI-PATIENT STUDY

PATIENT DATA

Participants
- 41 Normotensives
- 71 Hypertensives

Dataset
- Blood pressure
- Anatomic data from 3D TOF MR
- Flow data from PC-MR

MRI SEGMENTATION & CENTERLINE EXTRACTION

Vessels
- Right/left carotids (RC/LC)
- Right/left vertebrals (RV/LV)

Segmentation
MIMICS

Centerline extraction
VMTK

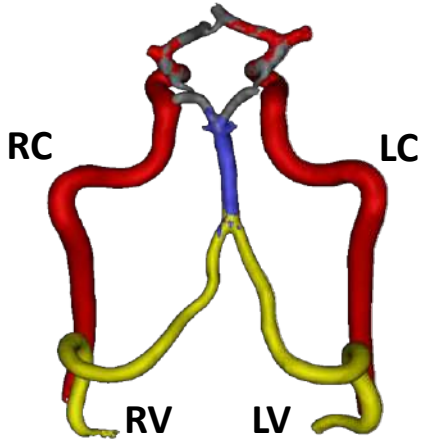

VASCULR SPLITTING & MORPHOMETRIC MEASUREMENT

Splitting
- 112/112 RC and LC
- 98/106 RV
- 101/106 LV

Measuring
Tortuosity, length and caliber

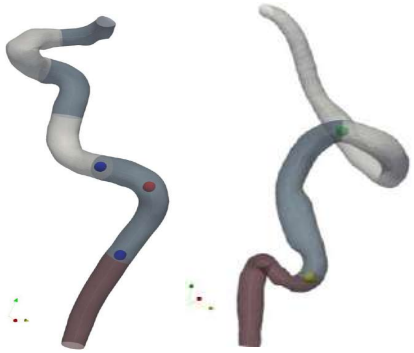

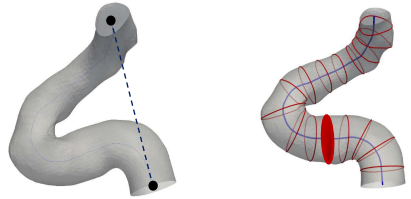

STATISTICAL ANALYSIS

Statistics:
- R (R Core Team 2013)
- Shapiro-Wilk test for normality check
- Unpaired t-test to compare means (paired to compare right/left sides)
- Wilcoxon test for not normally distributed variables
- CI = 95%, * $p<0.05$, ** $p<0.01$, *** $p<0.001$

RESULTS

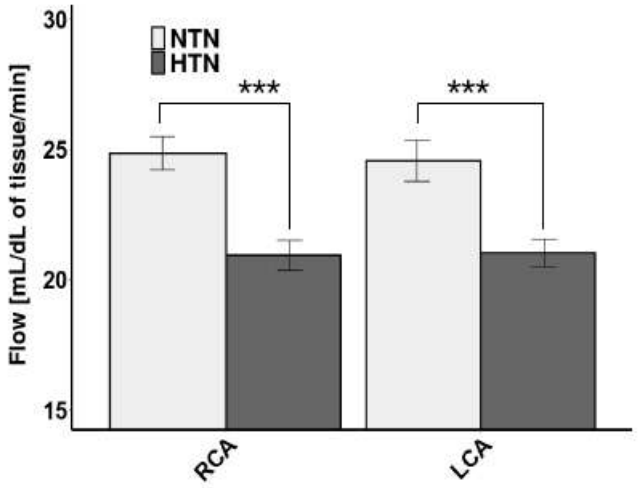

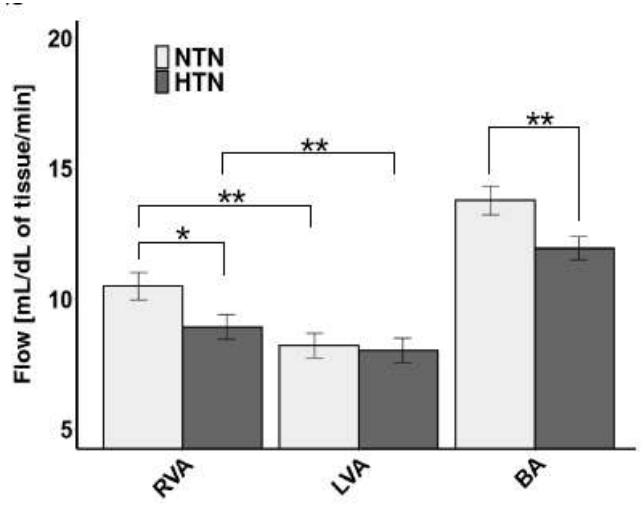

- In hypertensives, flow was lower in RCA, LCA, RVA but not in LVA
- Global and local morphometry of carotid arteries did not differ between hypertensives and normotensives
- Carotid flow did not correlate with morphometric features

- Hypertensives had longer and more tortuous RVA, but similar LVA
- Vertebral flow was negatively associated with length and cross-sectional area, but not with tortuosity

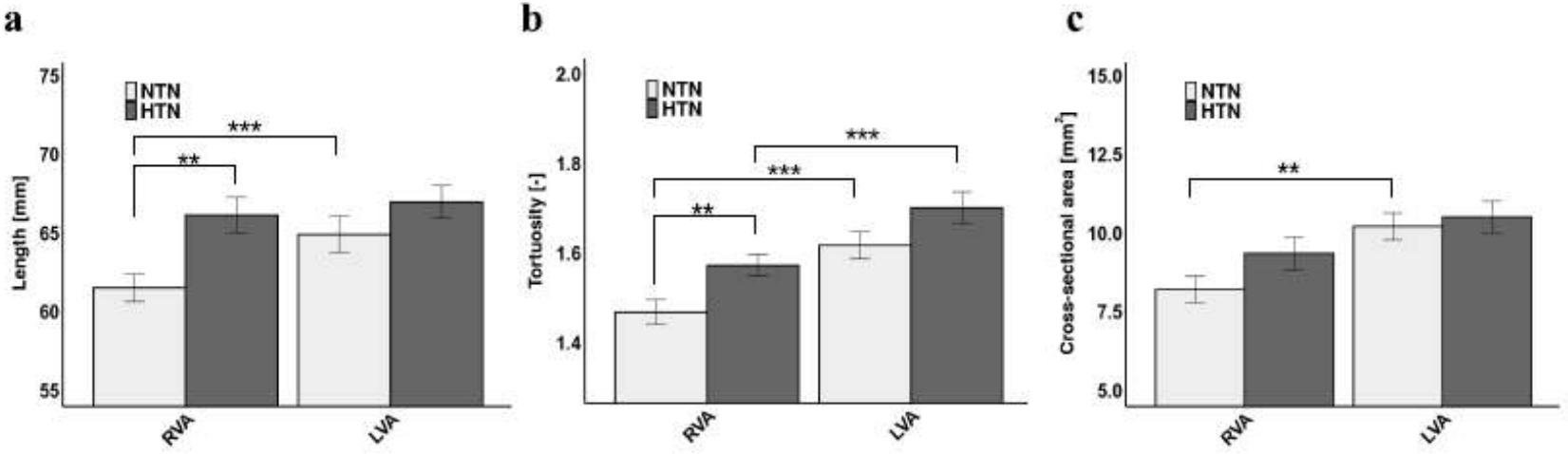

RCA=RIGHT CAROTID; **LCA**=LEFT CAROTID; **RVA**= RIGHT VERTEBRAL; **LVA**=LEFT VERTEBRAL; **BA**=BASILAR ARTERY

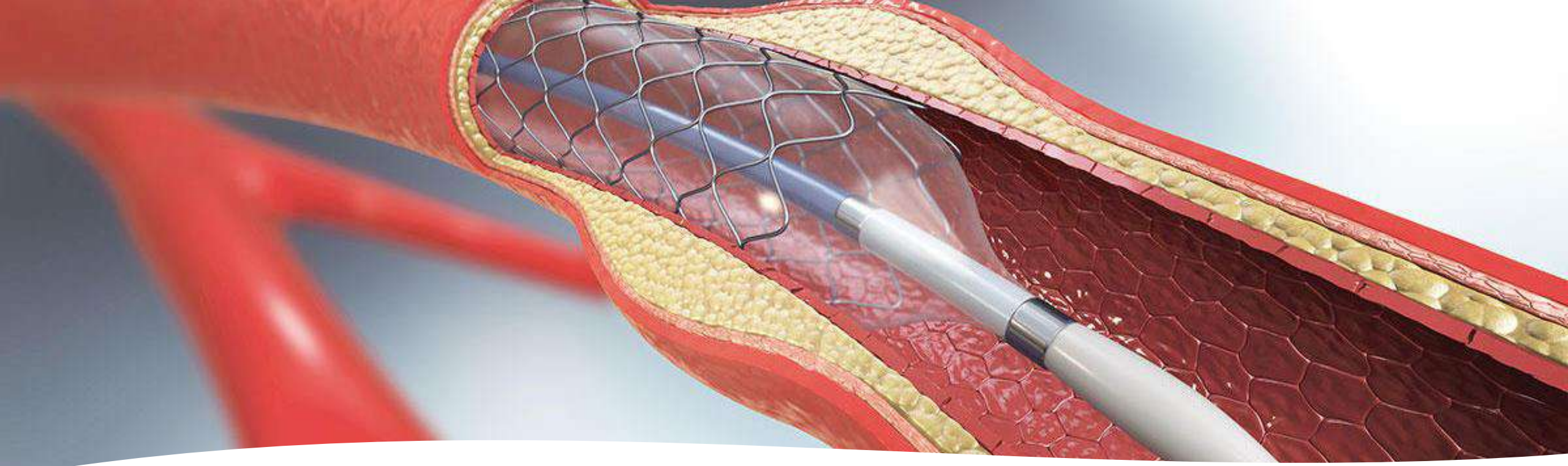

Carotid stenting, hemodynamics and restenosis

UNIVERSITÀ DI PAVIA

Los Alamos NATIONAL LABORATORY

Why hemodynamics after stenting?

- Stent implant leads to in-stent restenosis (ISR) through endothelial damage *(Koskinas et al. 2012)*
- Stent design influences flexibility, plaque coverage and flow (McClean et al. 2002)

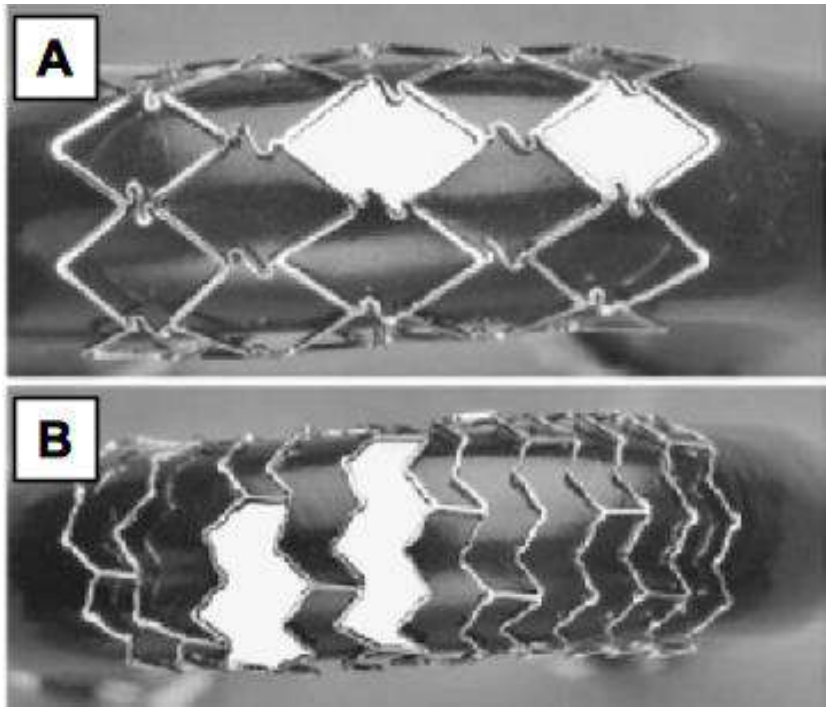

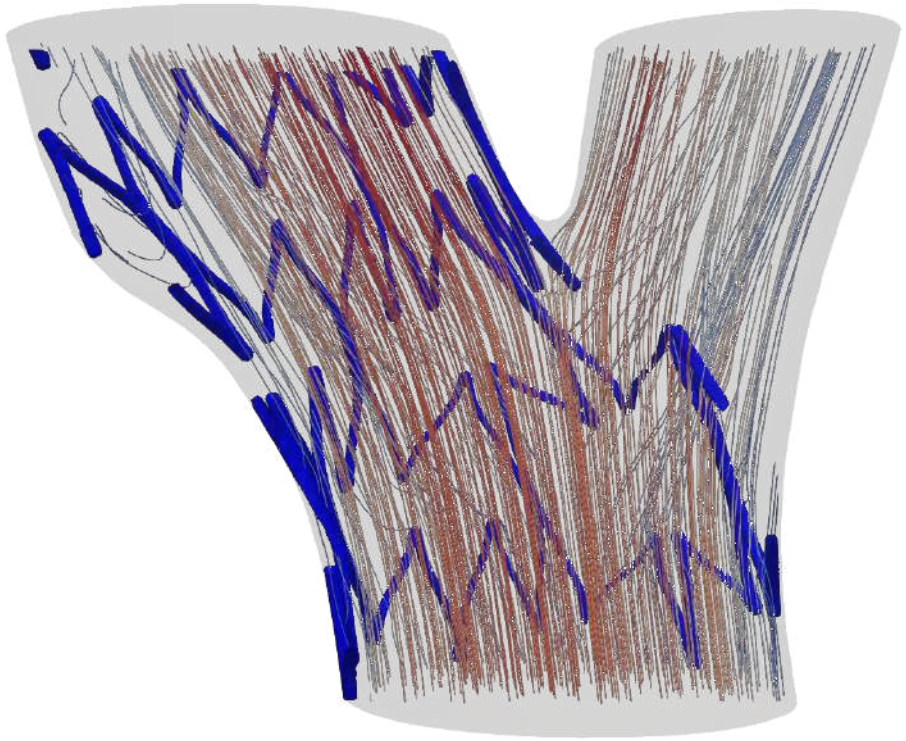

Why CFD?

- Superior spatio-temporal resolution than medical imaging/experimental techniques
- Predict flow in realistic/patient-specific models

BACKGROUND

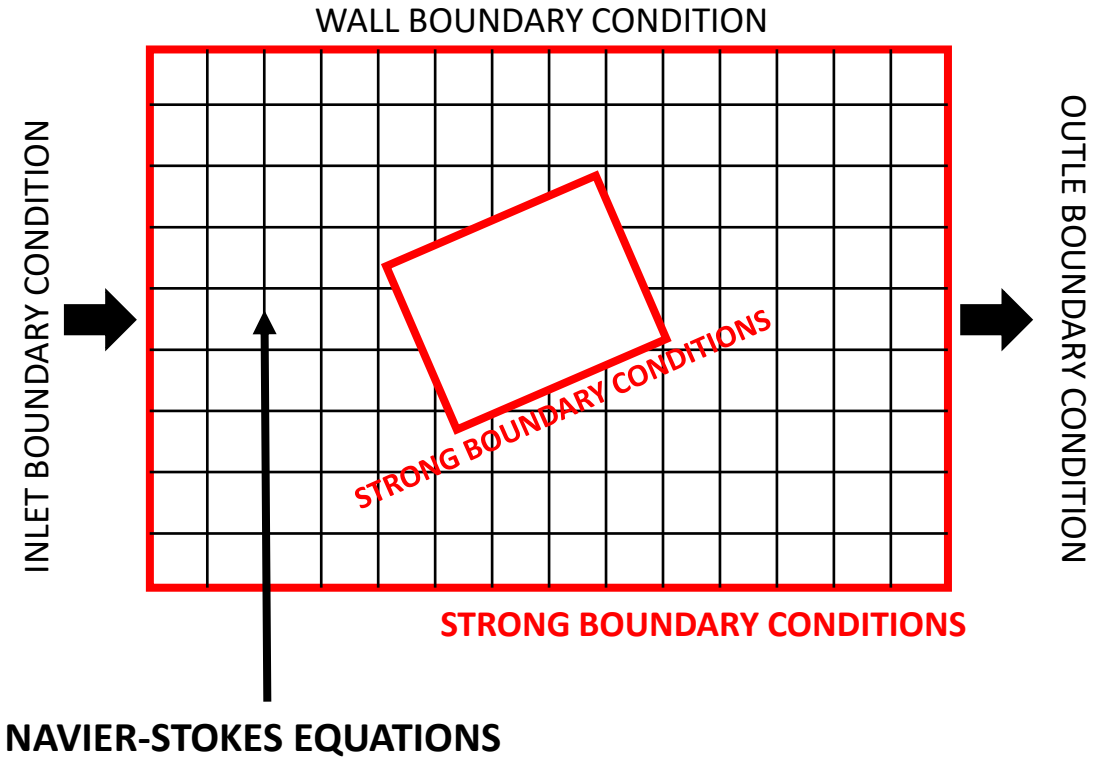

NEED A FAST MODEL SET-UP FOR CLINICAL USE

X Generation of computational grid by boolean operation is difficult due to thinness of stent struts

X Time-consuming model preparation

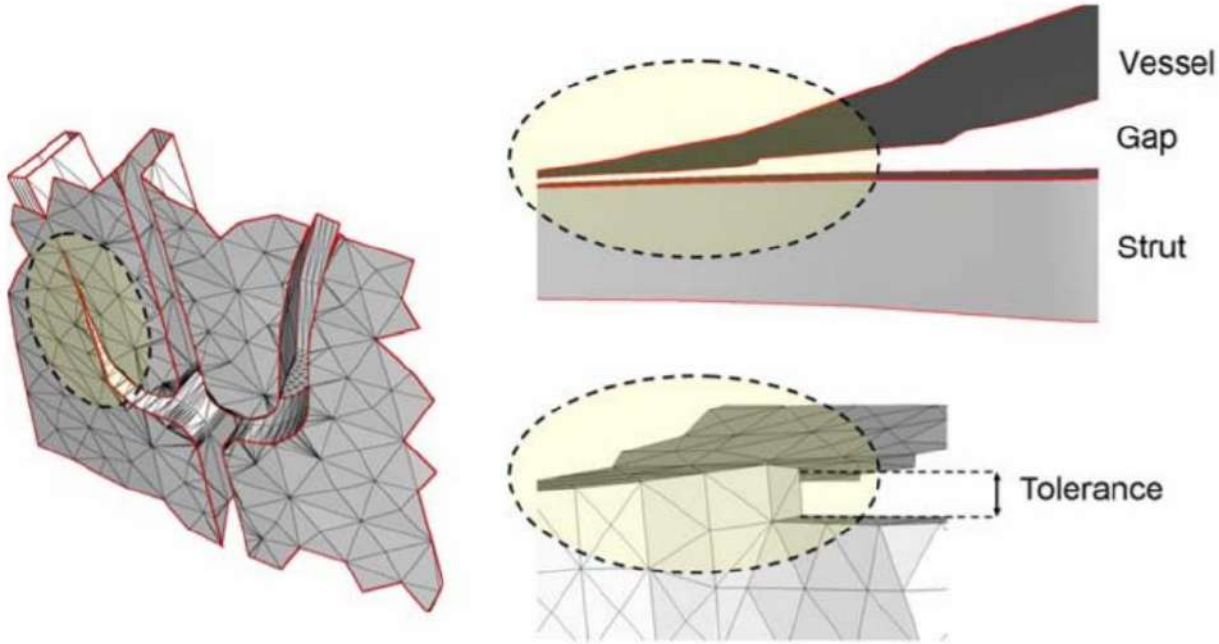

De Santis et al. 2013

AIM OF THE STUDY

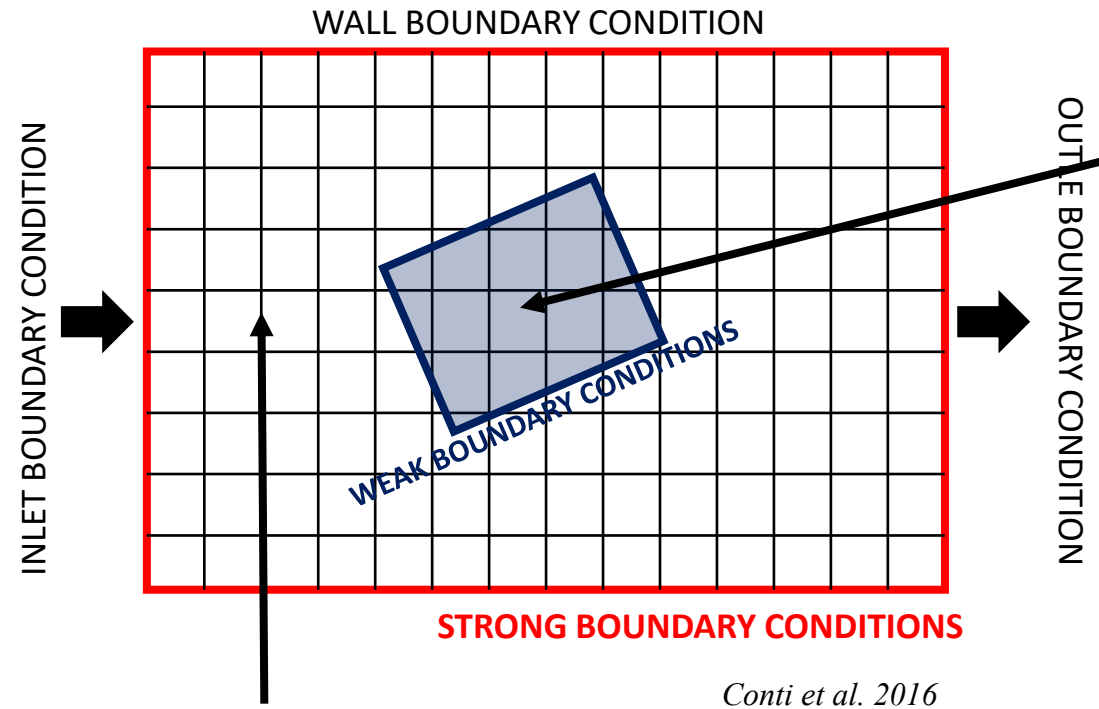

Conti et al. 2016

MODIFIED NAVIER-STOKES EQUATIONS

$$S_x = -KC(U_x - U_{x,solid})$$

$$S_y = -KC(U_y - U_{y,solid})$$

$$S_z = -KC(U_z - U_{z,solid})$$

EASIER MODELLING PREPARATION

WORSE SOLUTION ACCURACY

- Develop a framework to easily generate a **mesh refined** at the immersed boundary
- Set-up the CFD analysis by tuning the mesh and time parameters towards the target problem
- Compare post-stenting carotid hemodynamics with different stent designs
- Show an application of the developed framework in a proof-of-concept study

AUTOMATIC MESH REFINEMENT

INPUT

GEOMETRY STENT DEPLOYED (.STL)

GEOMETRY CAROTID POST-CAS (.STL)

CROP & REMESH

EXTRACT COORDINATES OF TRIANGLE NODES

MESH GENERATION WITH LOCAL REFINEMENT

NSE SOLUTION WITH IMMERSED APPROACH

FINITE ELEMENT STENT DEPLOYMENT

RIGID STENT DEPLOYMENT

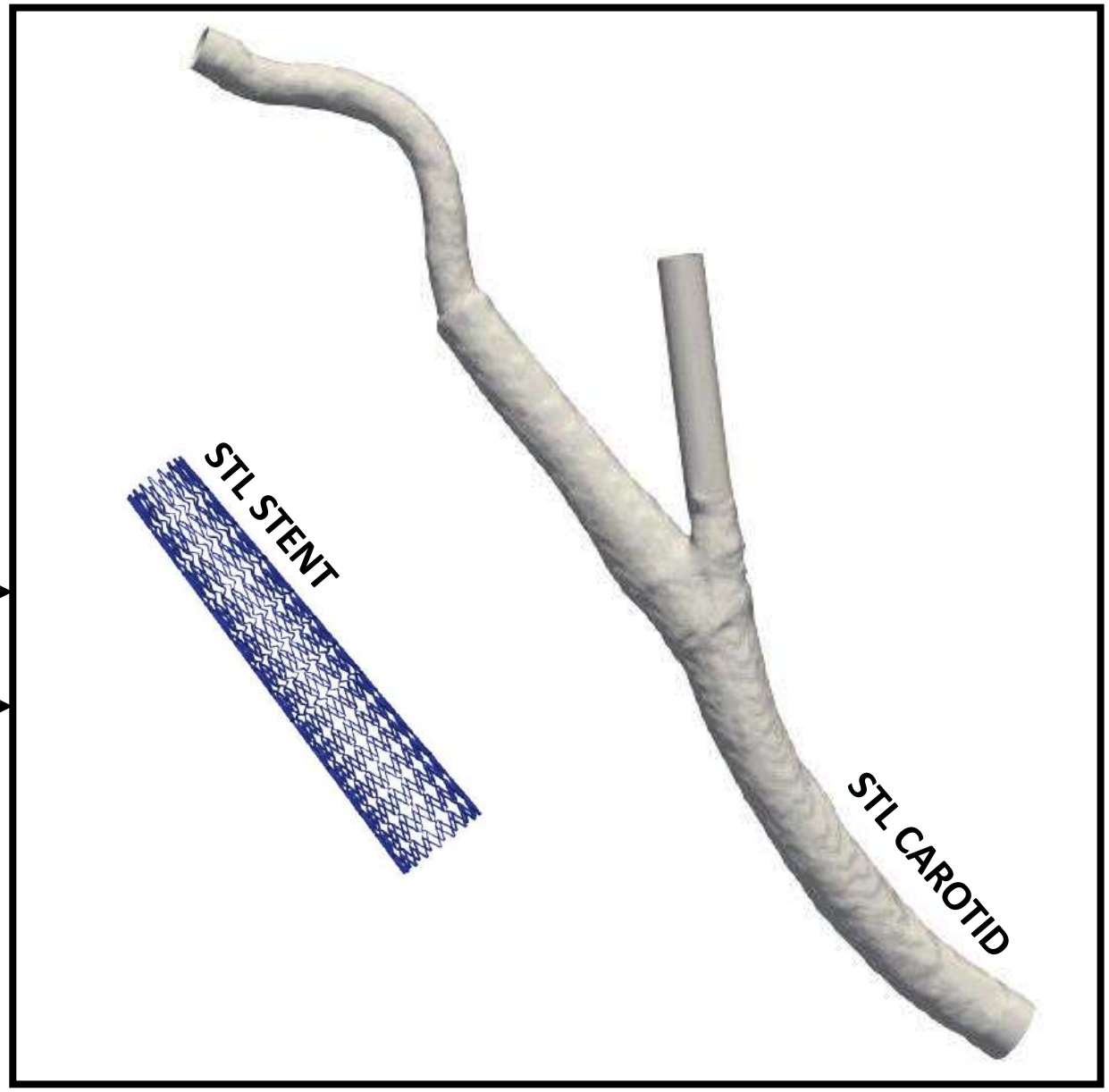

AUTOMATIC MESH REFINEMENT

GEOMETRY STENT DEPLOYED (.STL)

GEOMETRY CAROTID POST-CAS (.STL)

MESH REFINEMENT

CROP & REMESH

EXTRACT COORDINATES OF TRIANGLE NODES

MESH GENERATION WITH LOCAL REFINEMENT

NSE SOLUTION WITH IMMERSED APPROACH

CROP TO REFINE THE MESH ONLY NEAR SUBREGIONS OF THE STENT

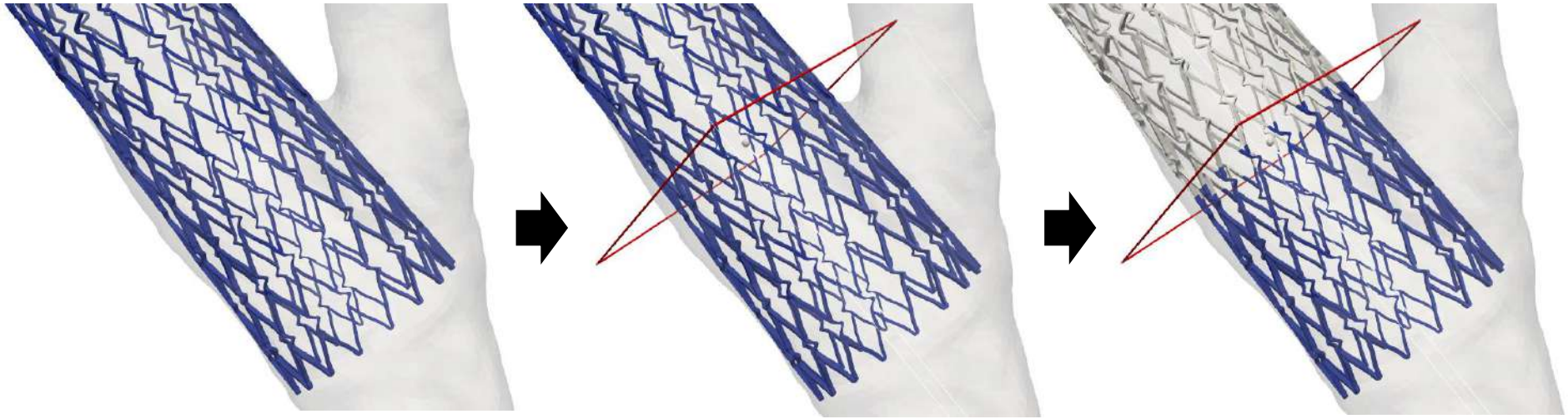

AUTOMATIC MESH REFINEMENT

GEOMETRY STENT DEPLOYED (.STL)

GEOMETRY CAROTID POST-CAS (.STL)

MESH REFINEMENT

CROP & REMESH

EXTRACT COORDINATES OF TRIANGLE NODES

MESH GENERATION WITH LOCAL REFINEMENT

NSE SOLUTION WITH IMMERSED APPROACH

CROP TO REFINE THE MESH ONLY NEAR SUBREGIONS OF THE STENT

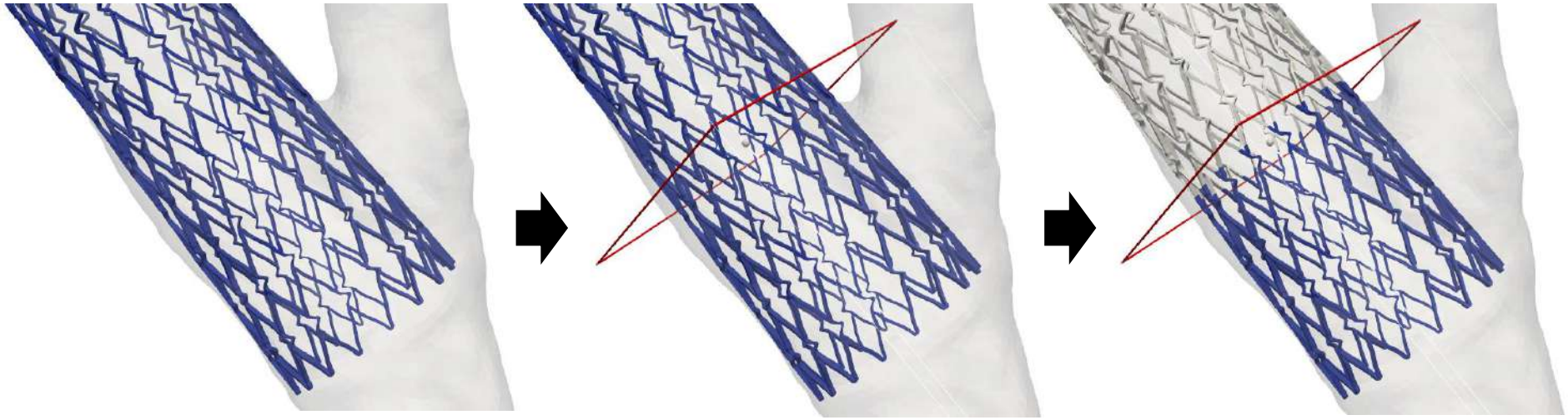

REMESH TO HAVE SUFFICIENTLY CLOSE TRIANGLE NODES

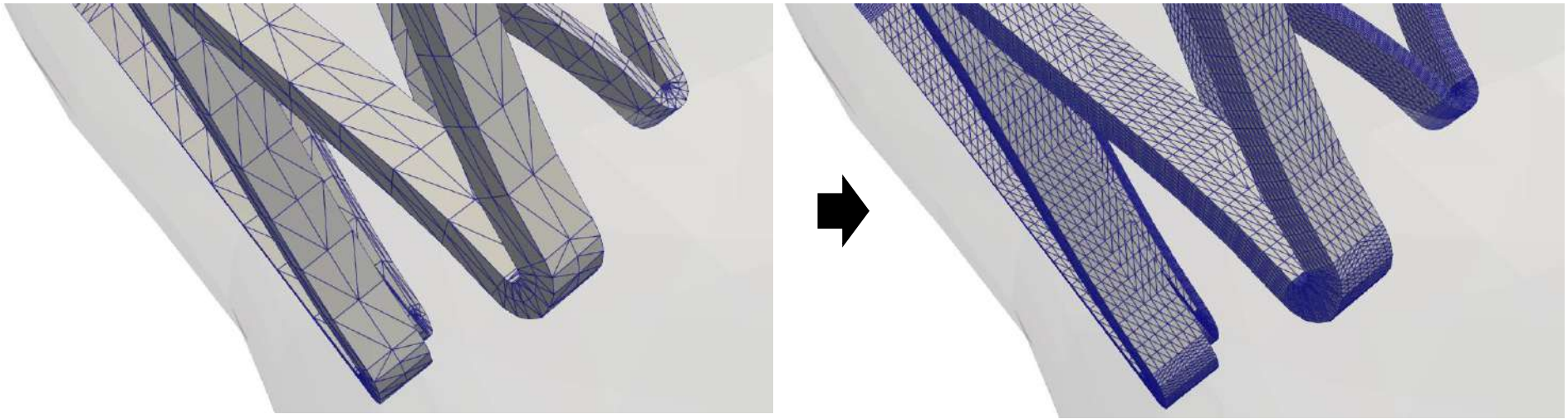

AUTOMATIC MESH REFINEMENT

GEOMETRY STENT DEPLOYED (.STL)

GEOMETRY CAROTID POST-CAS (.STL)

CROP & REMESH

EXTRACT COORDINATES OF TRIANGLE NODES

MESH GENERATION WITH LOCAL REFINEMENT

NSE SOLUTION WITH IMMERSED APPROACH

MESH REFINEMENT

EXTRACT THE COORDINATES OF THE TRIANGLE NODES THROUGH PYTHON SCRIPT

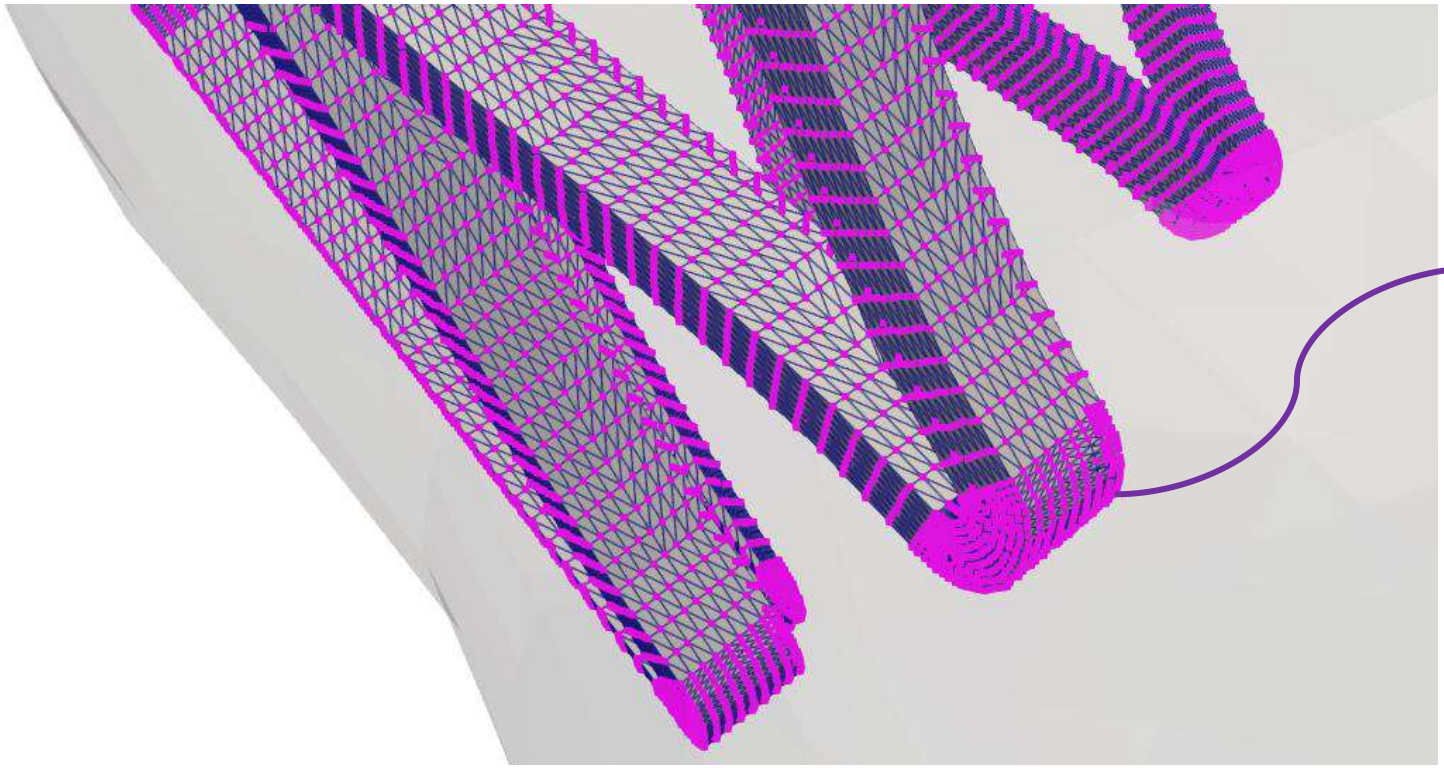

X	Y	Z
6.6233	2.33904	-9.62824
6.62416	2.33684	-9.64594
6.62657	2.3404	-9.64469
6.62067	2.33555	-9.62854
6.61606	2.34458	-9.62946
6.61925	2.34578	-9.64566
6.62203	2.3332	-9.64712
6.61831	2.33192	-9.62876
6.61081	2.33627	-9.63008
6.61439	2.33756	-9.64834
6.63104	2.34418	-9.66072
6.6289	2.34079	-9.66251
6.62368	2.3494	-9.66154
6.62698	2.33726	-9.66426
6.6193	2.34157	-9.66549
6.63438	2.34633	-9.67836
6.63639	2.3497	-9.6762
6.62897	2.3548	-9.67692

AUTOMATIC MESH REFINEMENT

GEOMETRY STENT DEPLOYED (.STL)

GEOMETRY CAROTID POST-CAS (.STL)

CROP & REMESH

EXTRACT COORDINATES OF TRIANGLE NODES

MESH GENERATION WITH LOCAL REFINEMENT

NSE SOLUTION WITH IMMERSED APPROACH

MESH REFINEMENT

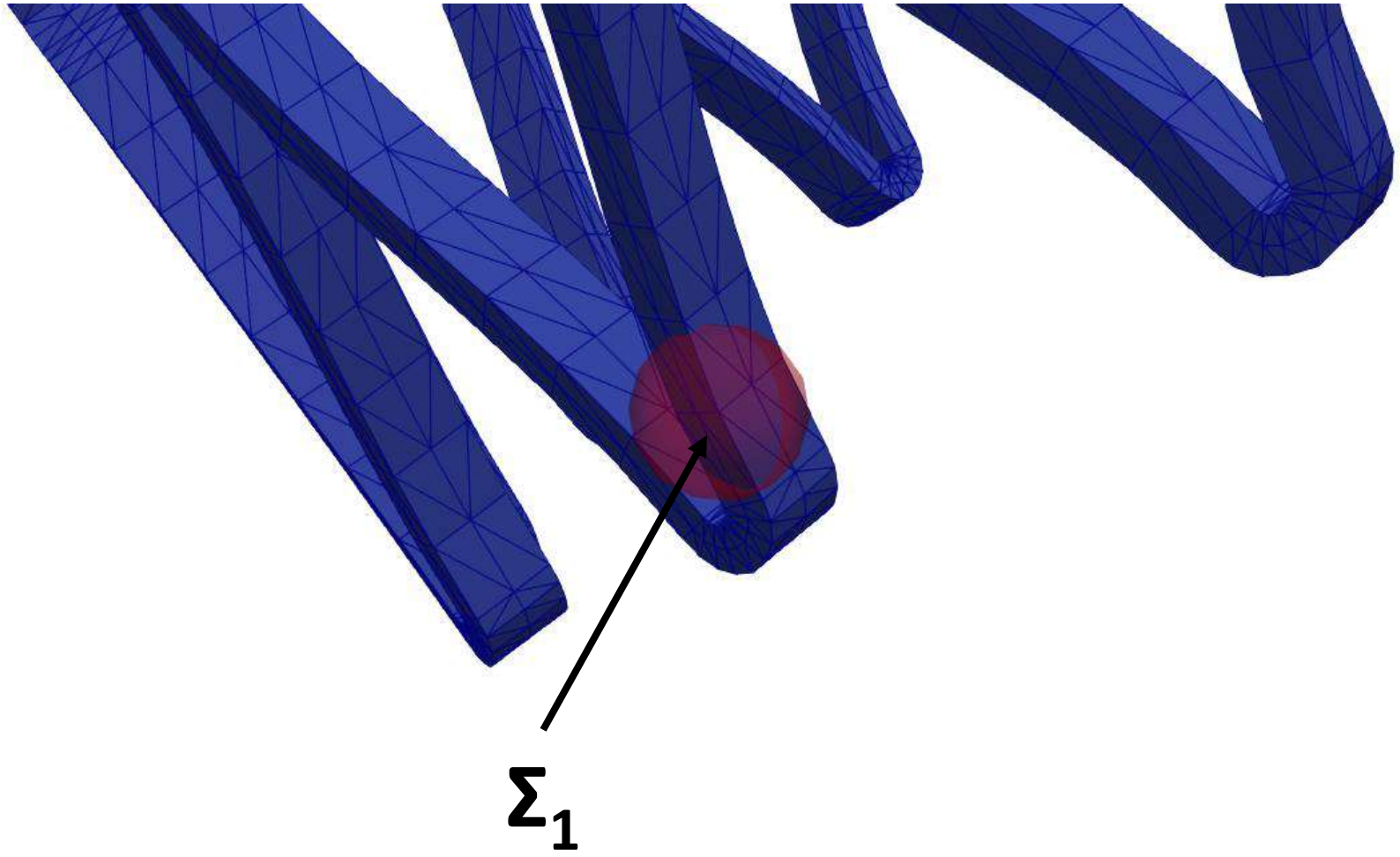

AUTOMATIC MESH REFINEMENT

GEOMETRY STENT DEPLOYED (.STL)

GEOMETRY CAROTID POST-CAS (.STL)

CROP & REMESH

EXTRACT COORDINATES OF TRIANGLE NODES

MESH GENERATION WITH LOCAL REFINEMENT

MESH REFINEMENT

NSE SOLUTION WITH IMMERSED APPROACH

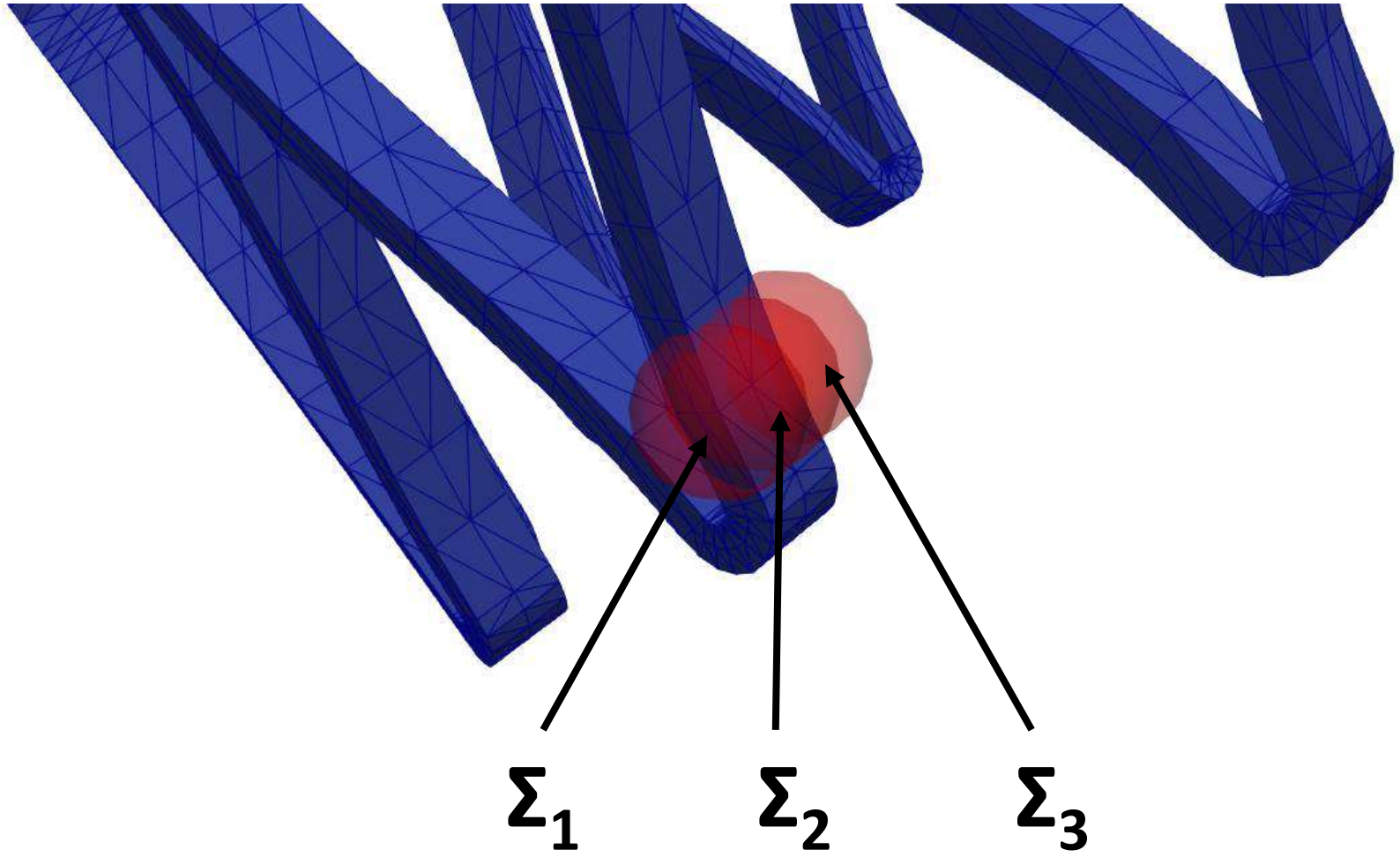

AUTOMATIC MESH REFINEMENT

GEOMETRY STENT DEPLOYED (.STL)

GEOMETRY CAROTID POST-CAS (.STL)

CROP & REMESH

EXTRACT COORDINATES OF TRIANGLE NODES

MESH GENERATION WITH LOCAL REFINEMENT

MESH REFINEMENT

NSE SOLUTION WITH IMMERSED APPROACH

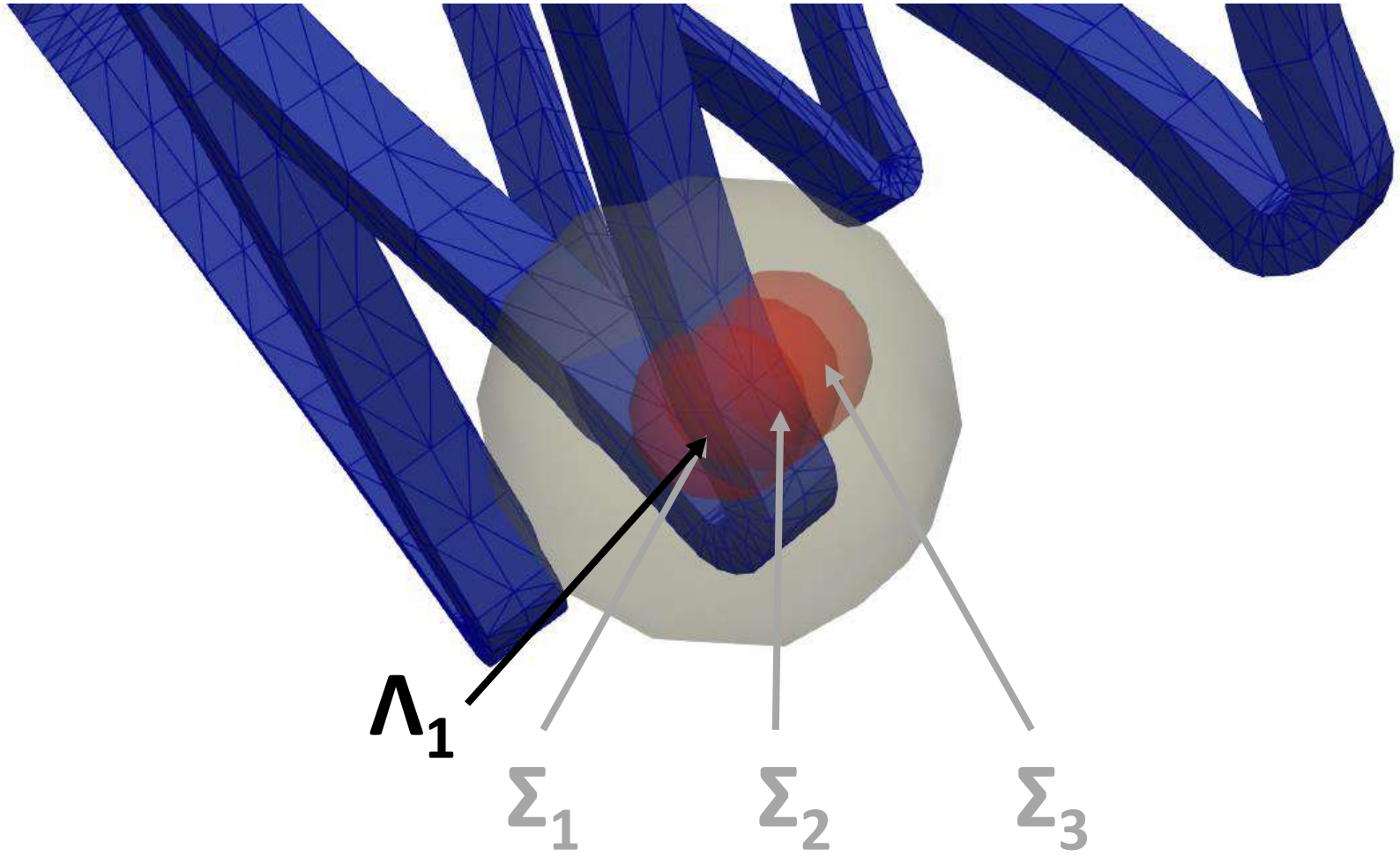

AUTOMATIC MESH REFINEMENT

GEOMETRY STENT DEPLOYED (.STL)

GEOMETRY CAROTID POST-CAS (.STL)

CROP & REMESH

EXTRACT COORDINATES OF TRIANGLE NODES

MESH GENERATION WITH LOCAL REFINEMENT

NSE SOLUTION WITH IMMERSED APPROACH

MESH REFINEMENT

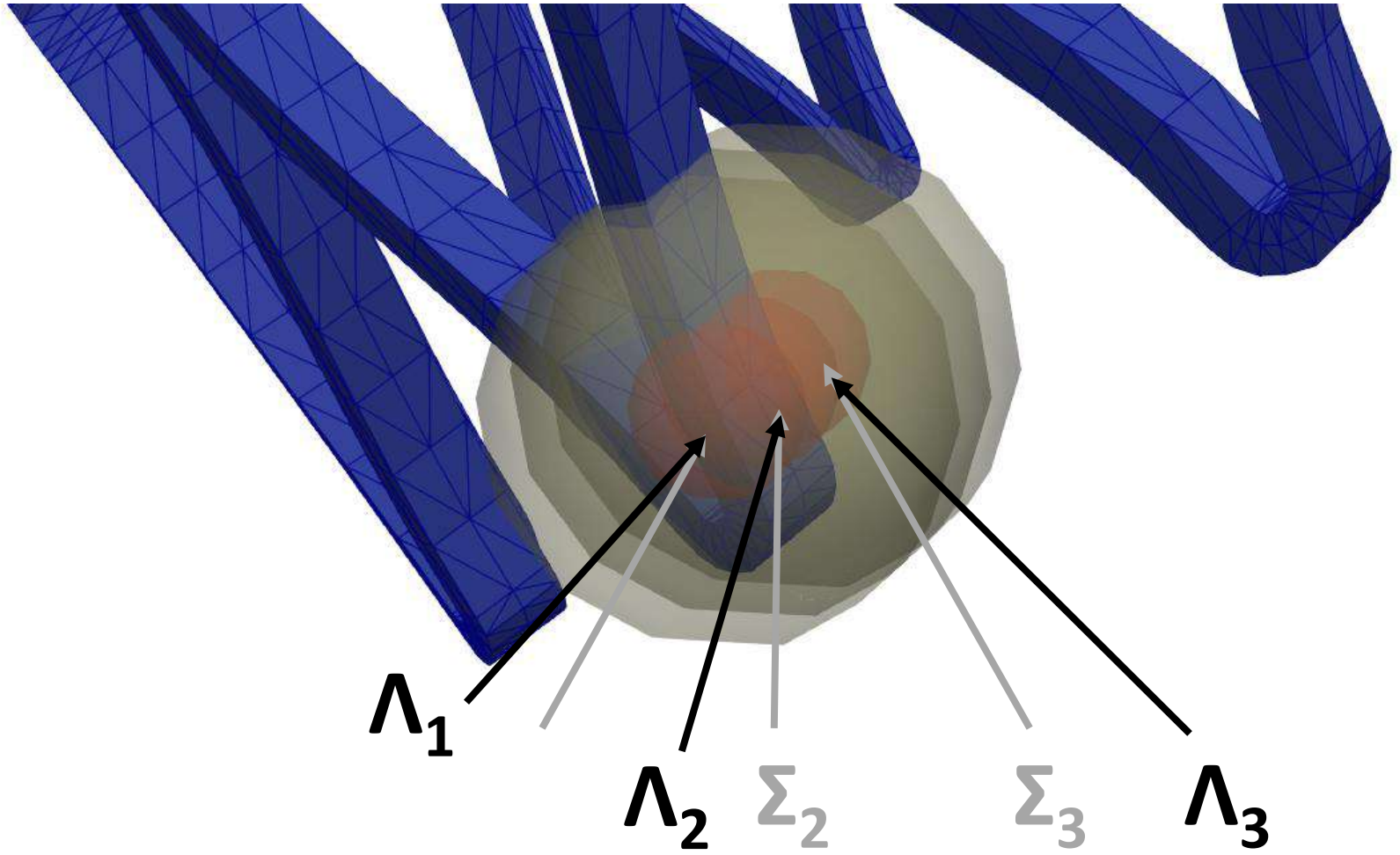

AUTOMATIC MESH REFINEMENT

GEOMETRY STENT DEPLOYED (.STL)

GEOMETRY CAROTID POST-CAS (.STL)

CROP & REMESH

EXTRACT COORDINATES OF TRIANGLE NODES

MESH GENERATION WITH LOCAL REFINEMENT

MESH REFINEMENT

NSE SOLUTION WITH IMMERSED APPROACH

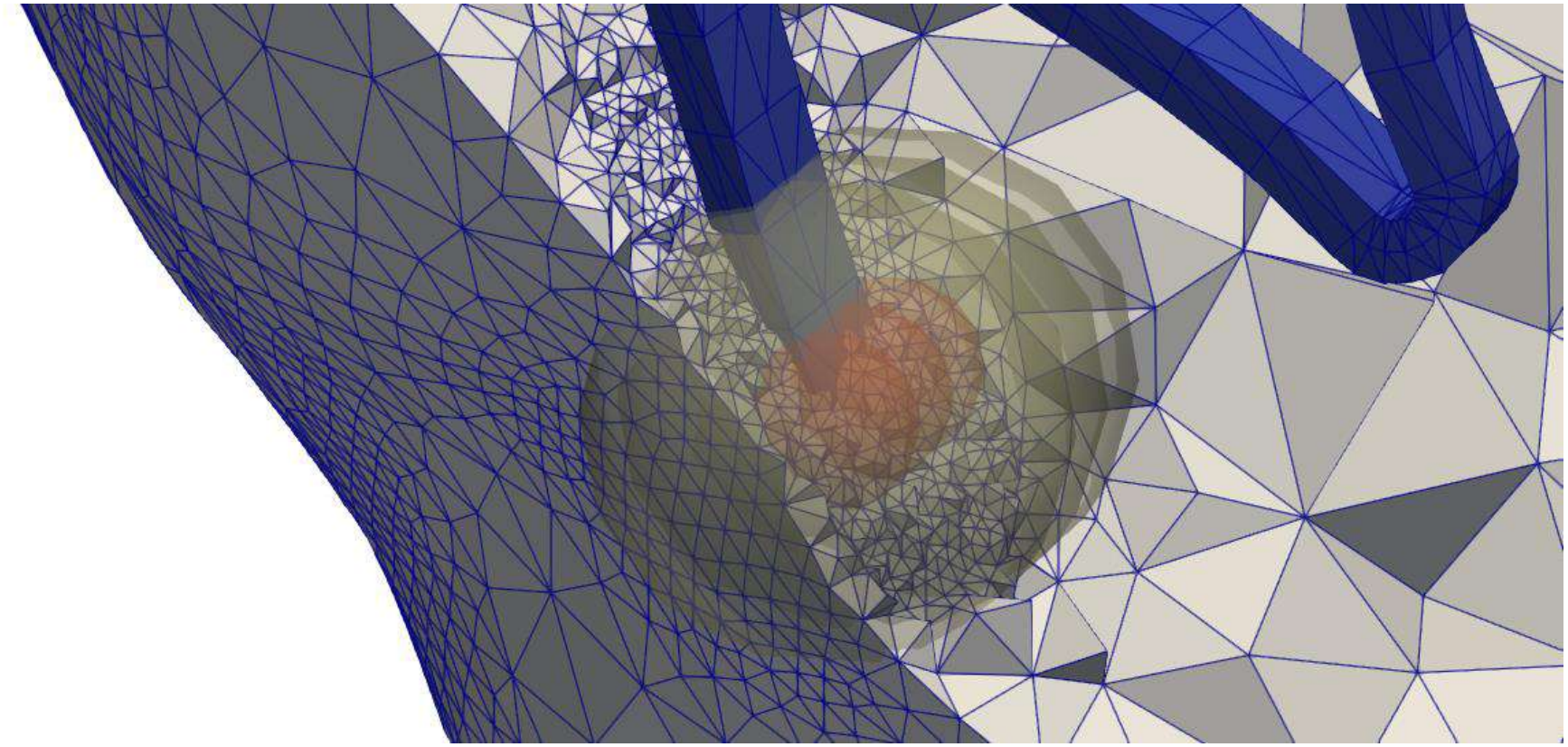

MESH CALIBRATION: IDEALIZED MODEL

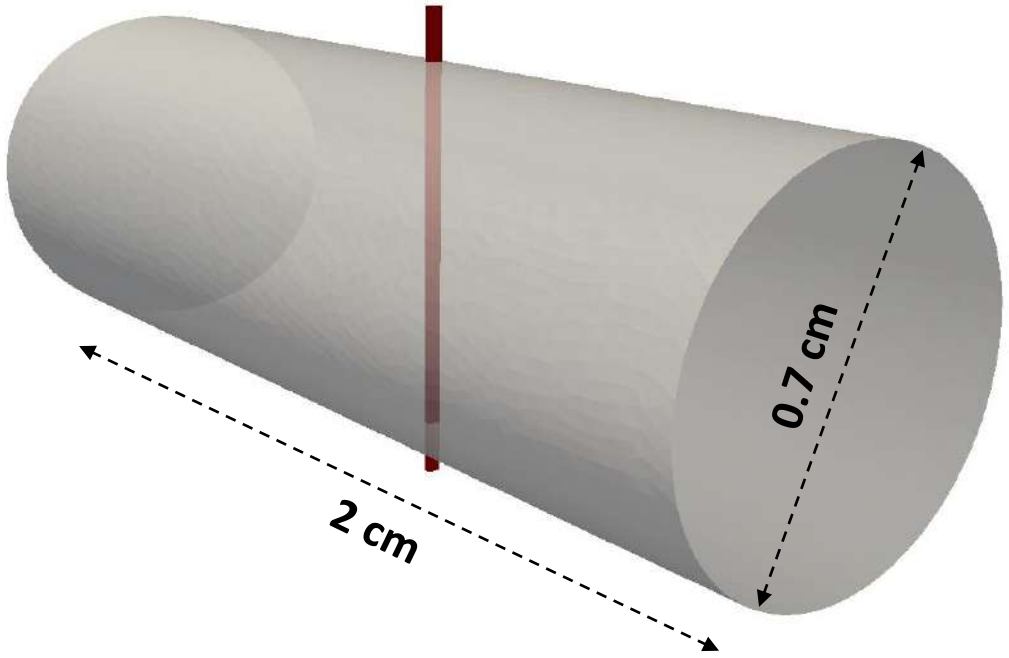

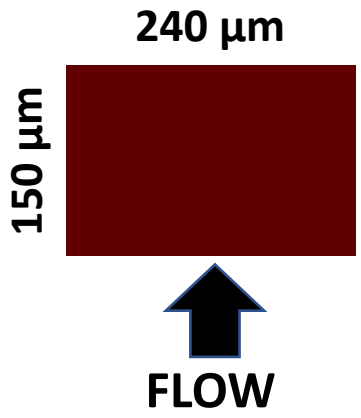

- Idealized model of stent strut immersed in a cylindrical artery
- Assess two mesh sizes: refined and unrefined regions
- Comparison between body-fitted and immersed meshes

COARSE REGION

Edge length [µm]	Body-fitted [#DOF]	Immersed [#DOF]
400	19798	19448
300	44865	44756
200	146302	146258
100	1131822	1145806

REFINED REGION

Edge length [µm]	Body-fitted [#DOF]	Immersed [#DOF]
50	201663	191392
25	472629	418570
18.75	687250	576709
12.5	1164805	892674

MESH CALIBRATION: VELOCITY RESULTS

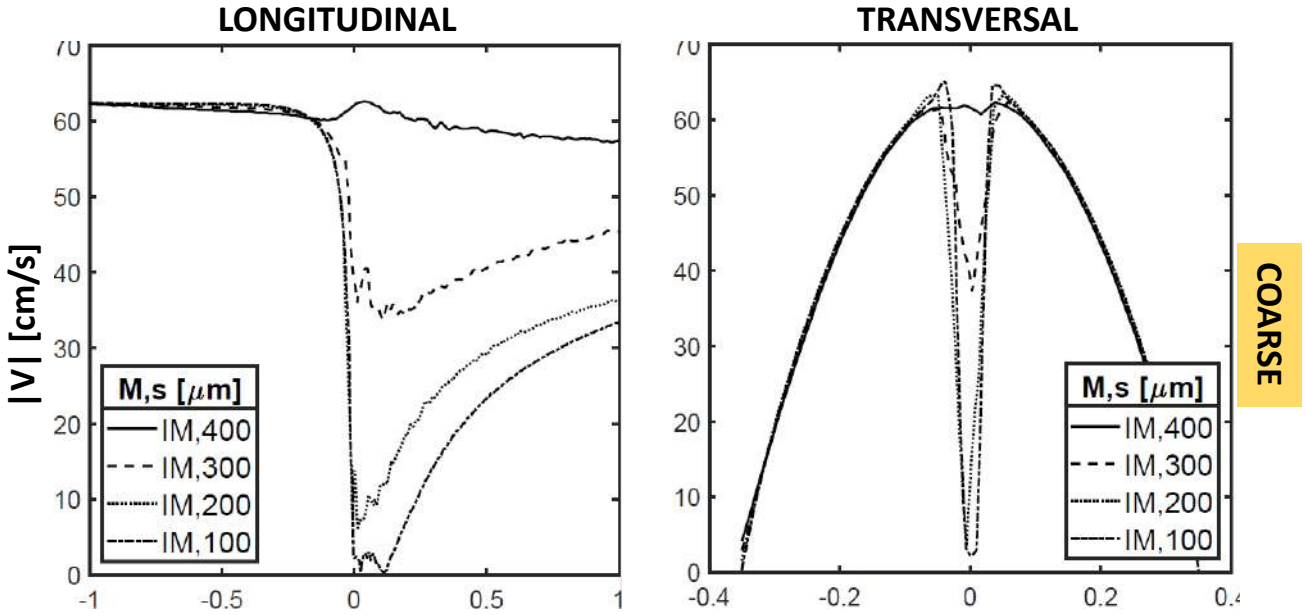

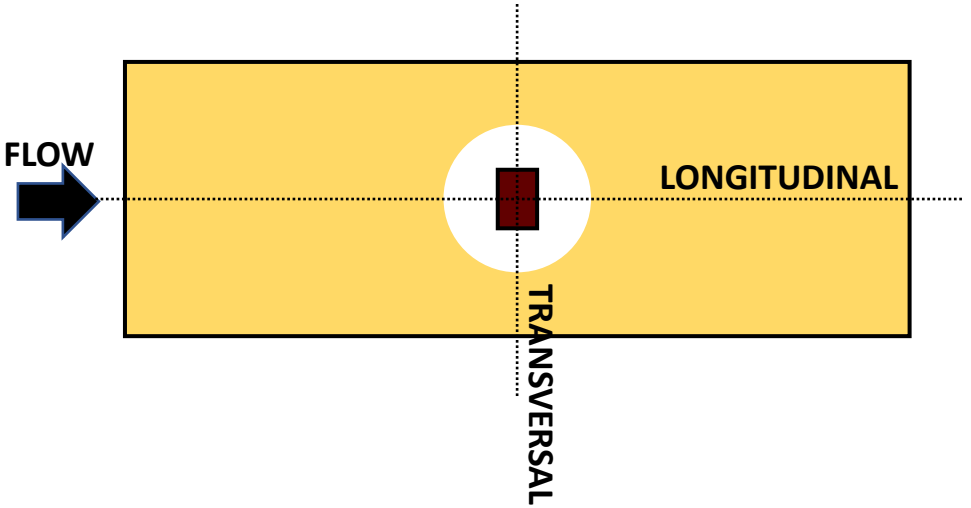

RESULTS

- Element size of 300 μm in the **unrefined** region

MESH CALIBRATION: VELOCITY RESULTS

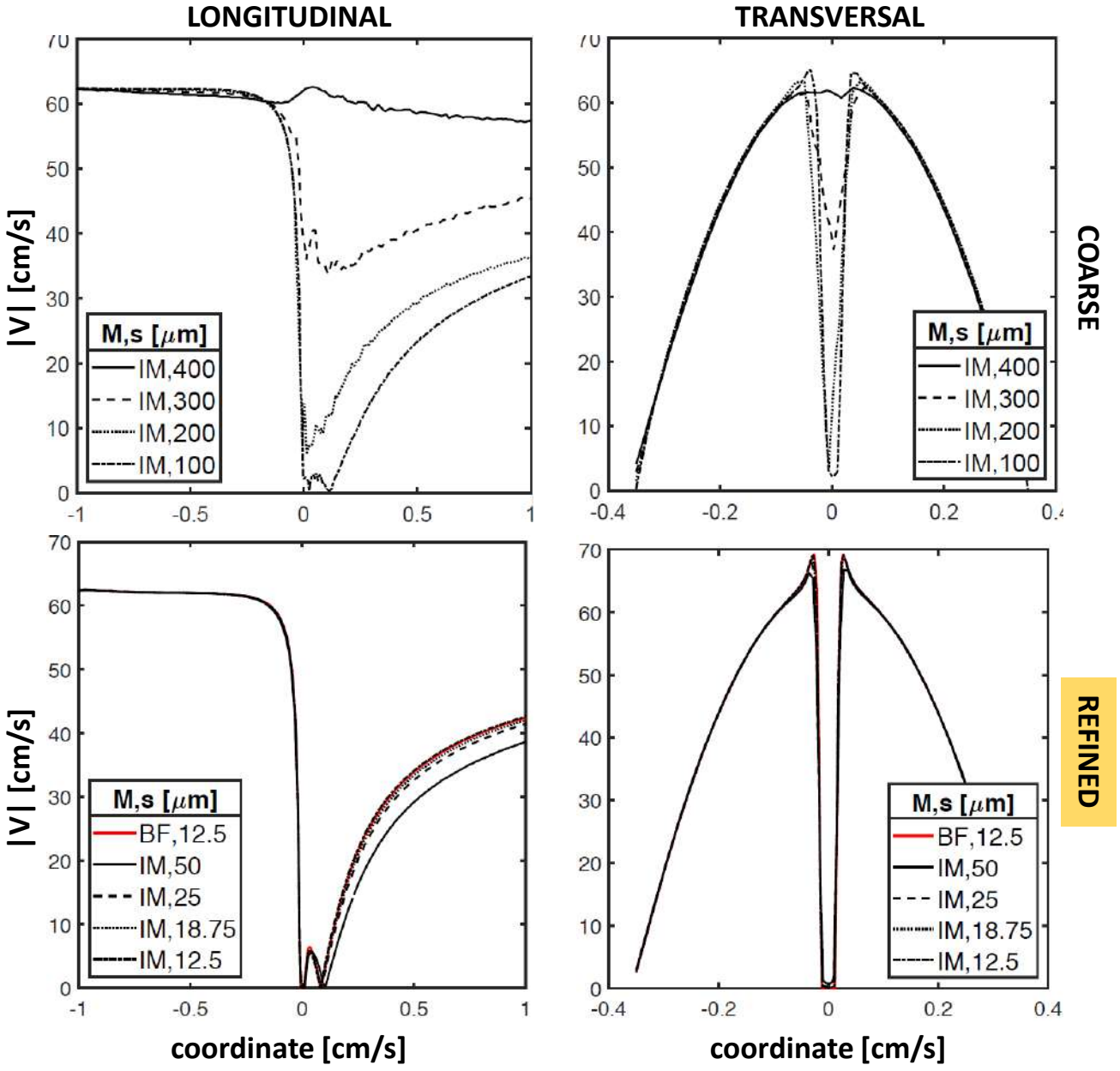

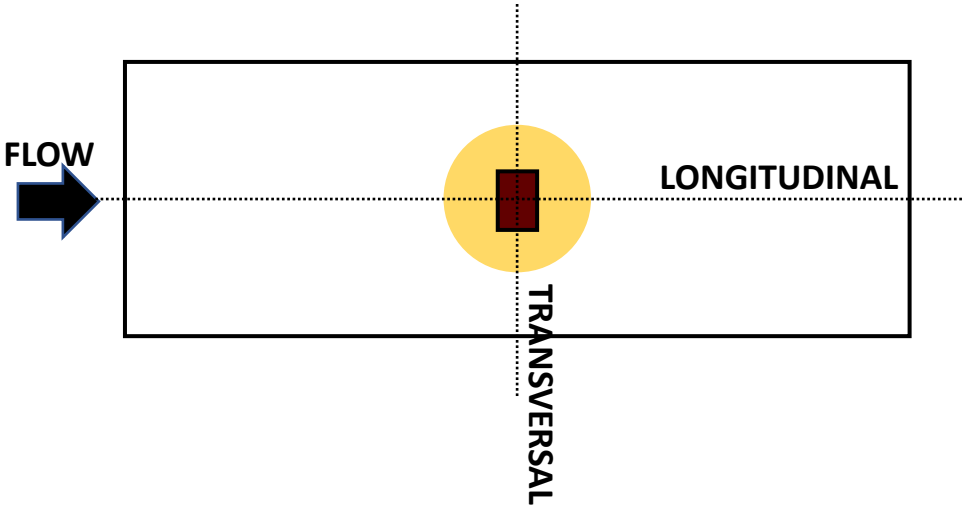

RESULTS

- Element size of 300 μm in the **unrefined** region
- Element size 25 μm in the **refined** region
- Growth rate of 1.2 in the **transition** zone

MESH CALIBRATION: WSS RESULTS

AXIS A

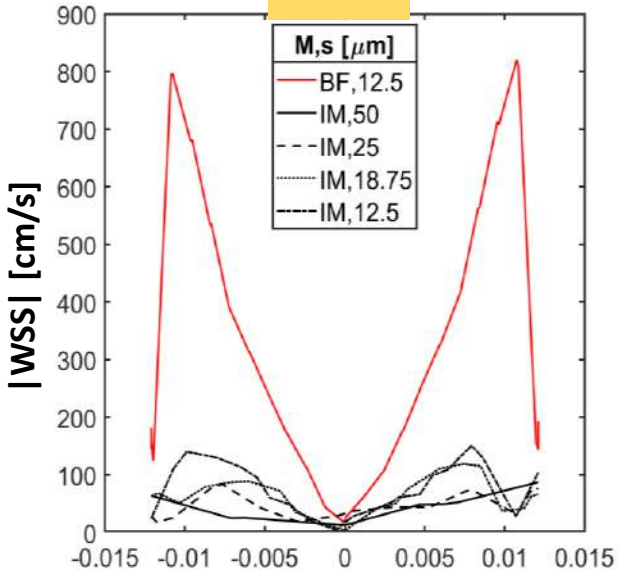

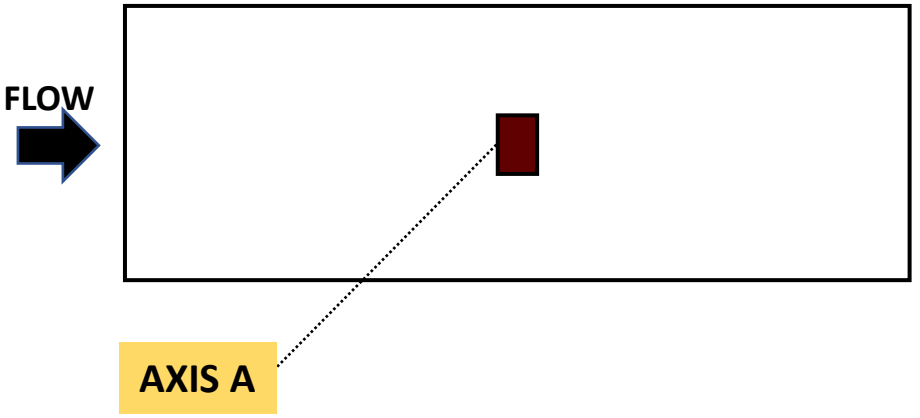

MESH CALIBRATION: WSS RESULTS

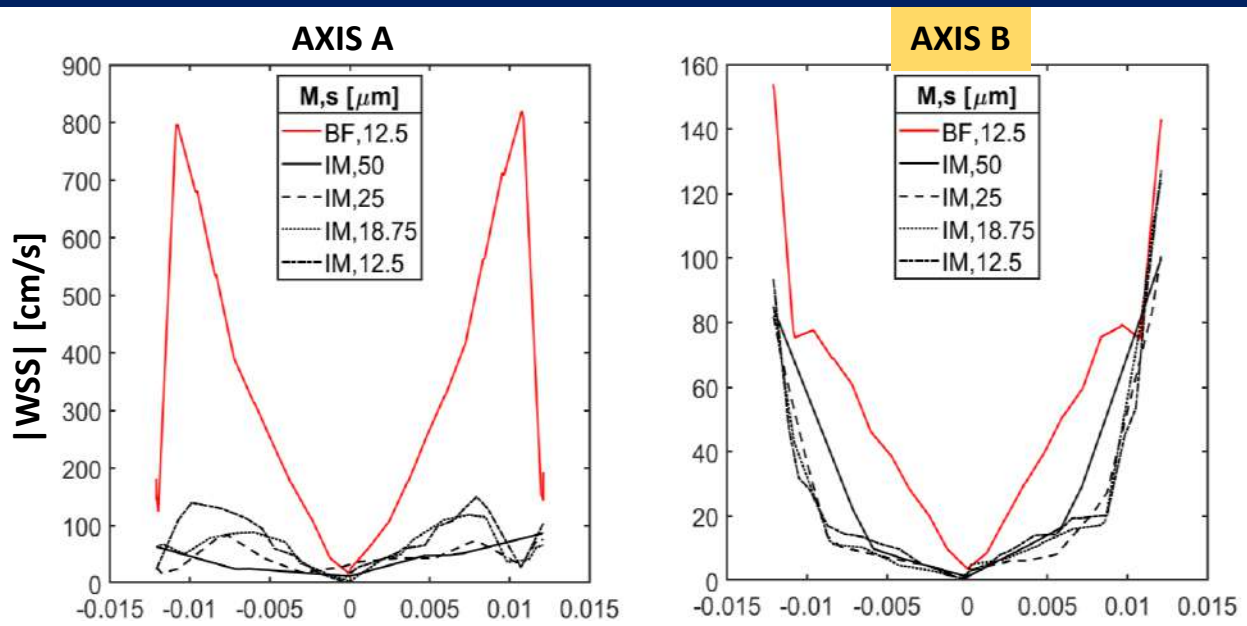

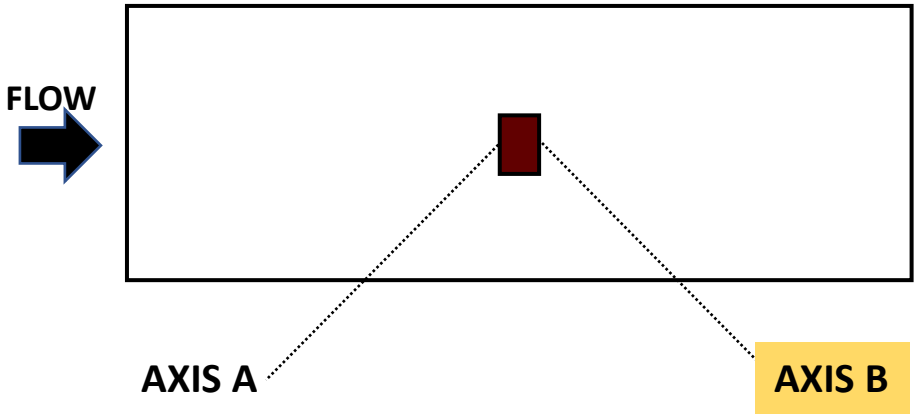

MESH CALIBRATION: WSS RESULTS

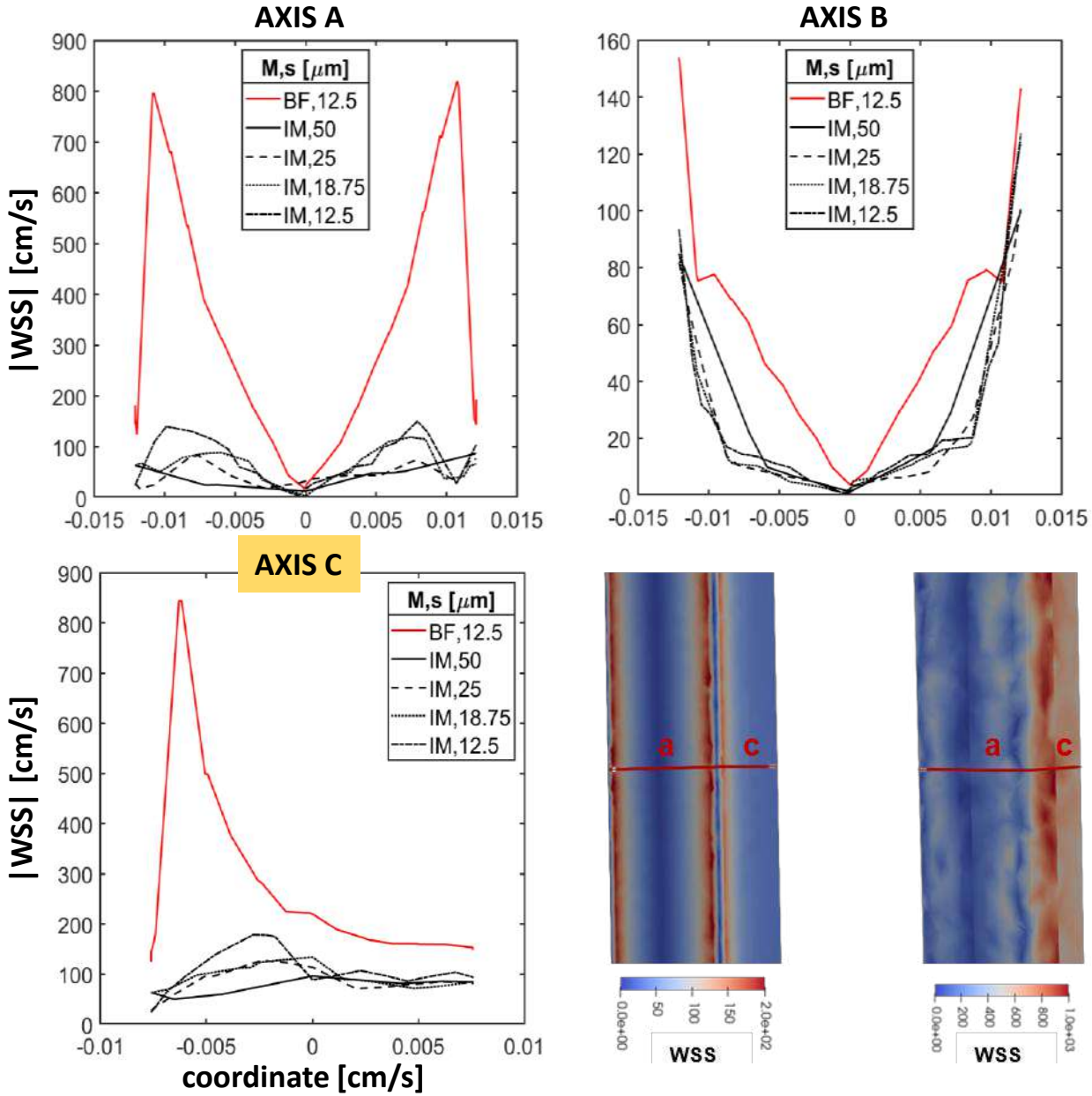

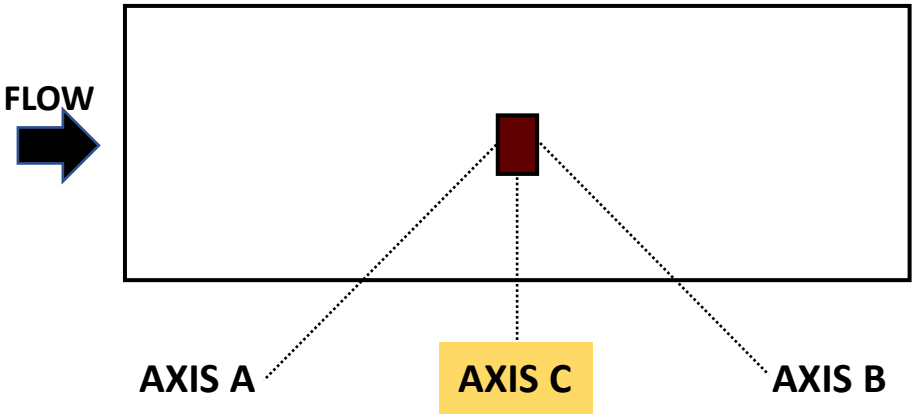

RESULTS

- WALL SHEAR STRESS (WSS) are less accurate
- No improvement with mesh size

POST-STENTING BLOOD FLOW: COMPARATIVE STUDY

POST-STENTING CAROTID AND STENT GEOMETRIES

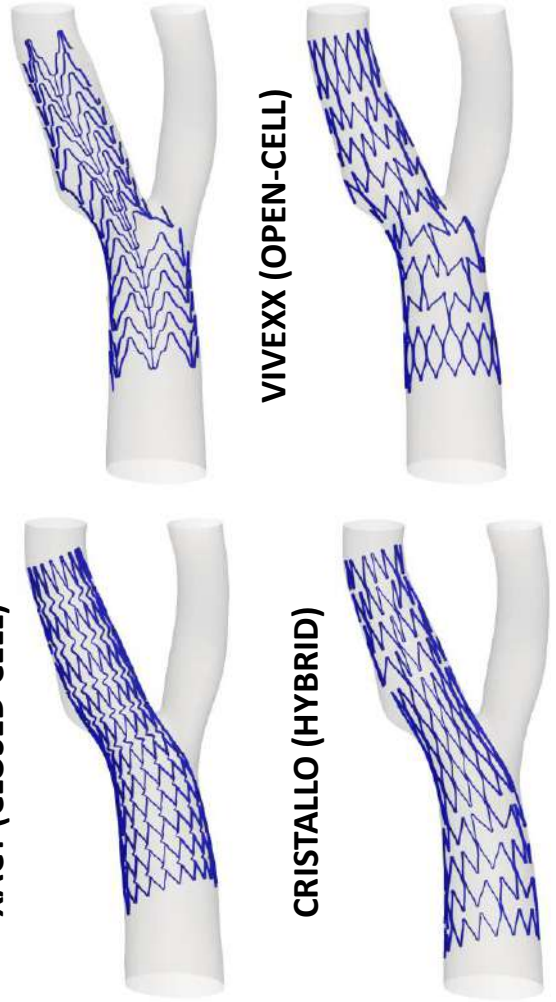

MESH GENERATION WITH LOCAL REFINEMENT

Element size

- **100 µm** in the stented region
- **25 µm** in a stent subregion at bifurcation

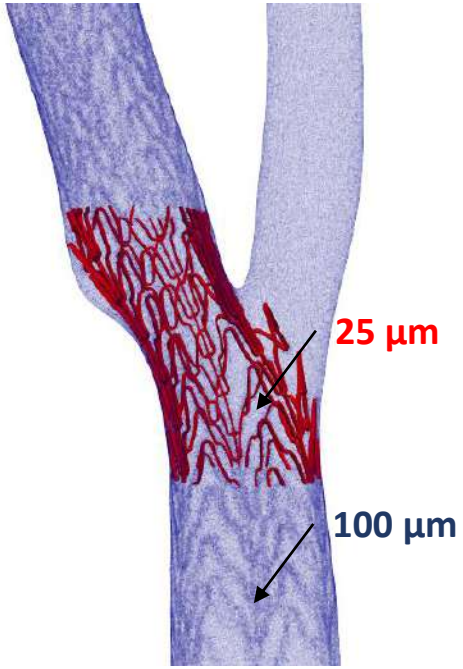

CFD SET-UP

Modelling assumptions

- Flow split ICA/ECA
- Zero traction outlet
- Laminar
- Newtonian blood

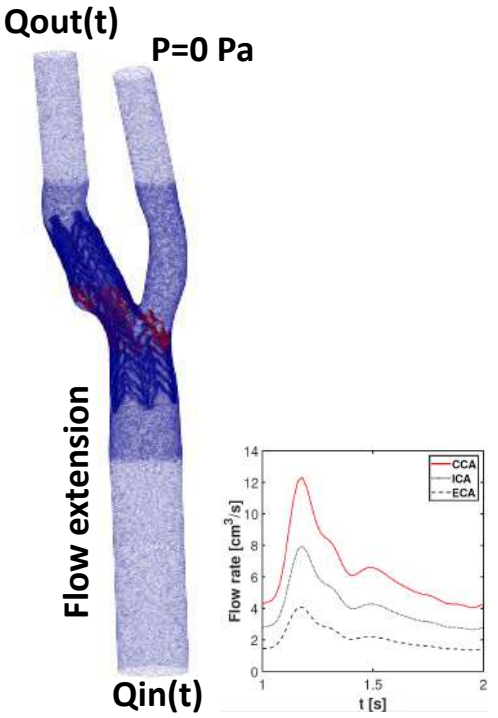

POST-PROCESSING THROUGH HEMODYNAMIC INDECES

- **Velocity streamline**
- **Time Averaged Wall Shear Stress**
  < 4 dyne/cm2 → ISR
- **Vascular resistance:**
  $R_{ICA}=(P_{CCA}-P_{ICA})/(Q_{ICA})$
  $R_{ECA}=(P_{CCA}-P_{ECA})/(Q_{ECA})$

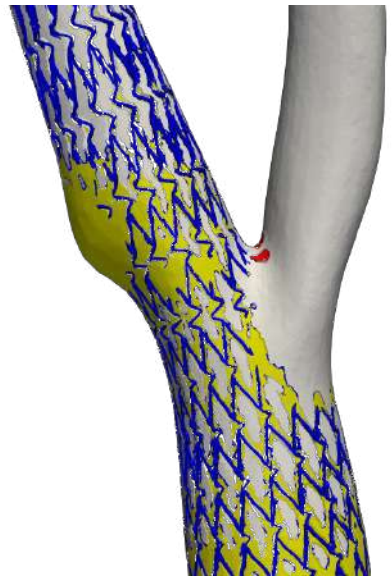

RESULTS

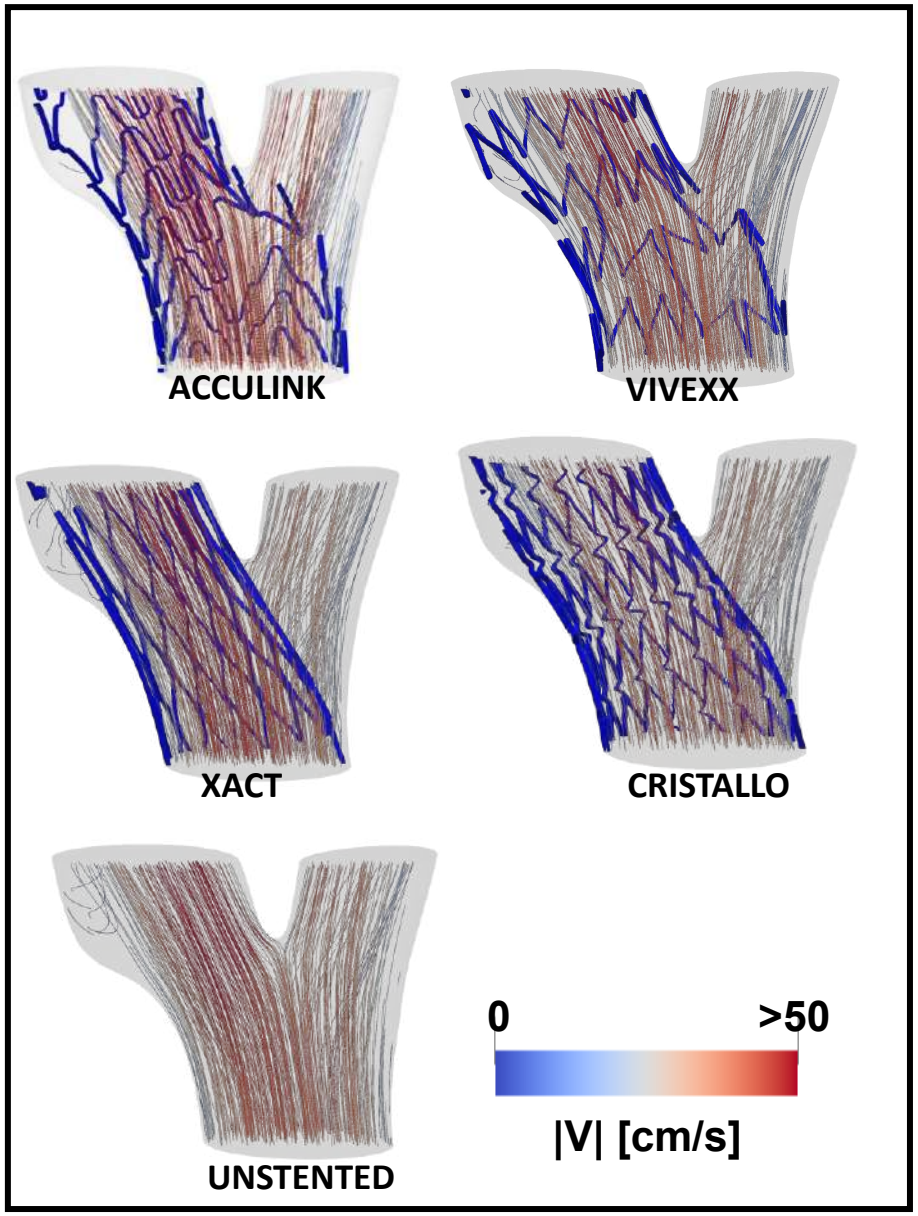

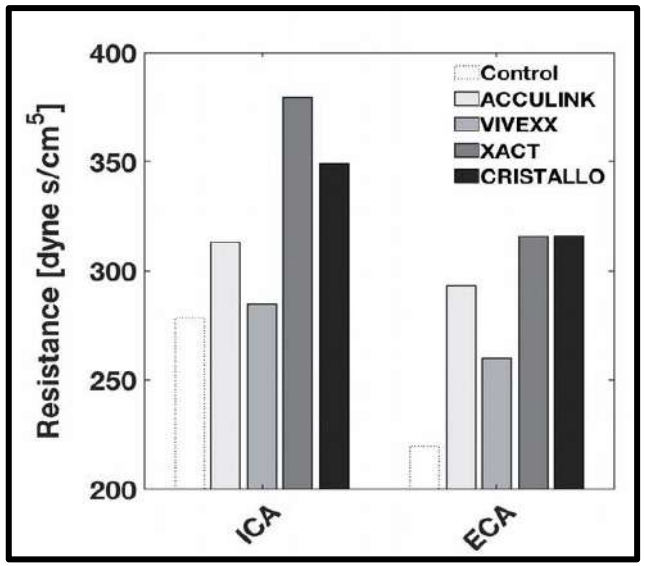

RESULTS

- No significant alteration of flow pattern around thin stent struts
- Increased low TAWSS area
- Increased ECA resistance (closed-cell)

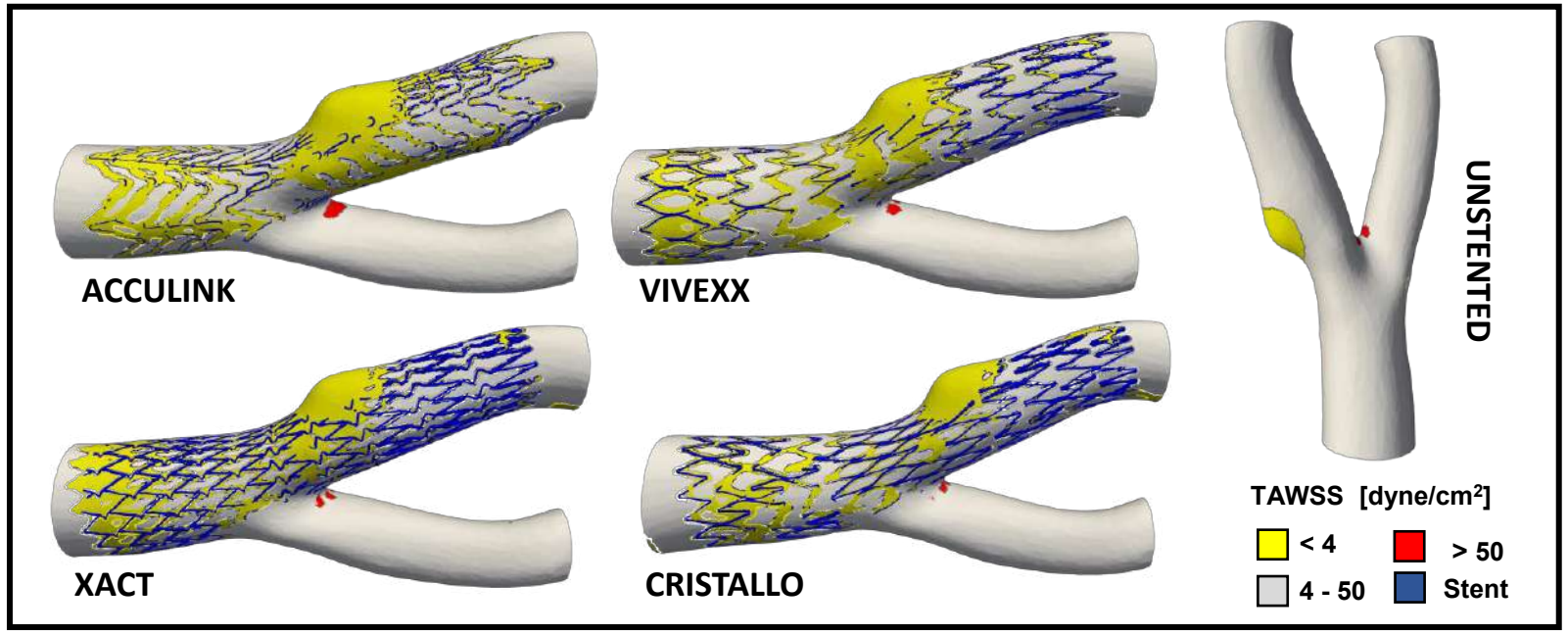

CONCLUSIONS AND FUTURE PERSPECTIVES

- Implemented computational frameworks to investigate geometrical and hemodynamic aspects of carotid artery
- Applied the morphometric framework in a multi-patient study to automatically extract morphometric measures
- Applied the hemodynamic framework in a proof-of-concept study comparing different stent designs

- Increase automatization of morphometric framework (segmentation, splitting)
- Improve WSS accuracy of hemodynamic framework (forcing parameter)
- Validate hemodynamic framework (numerically/experimentally)
- Apply hemodynamic framework on a multi-patient study

I.R.C.C.S. POLICLINICO SAN DONATO

REFERENCES

Michele **Conti**, Chris Long, Michele Marconi, Raffaella Berchiolli, Yuri Bazilevs, and Alessandro Reali. Carotid artery hemodynamics before and after stenting: A patient specific cfd study. Computers & Fluids, 141:62–74, 2016.

Gianluca **De Santis**, Michele Conti, Bram Trachet, Thomas De Schryver, Matthieu De Beule, Joris Degroote, Jan Vierendeels, Ferdinando Auricchio, Patrick Segers, Pascal Verdonck, et al. Haemodynamic impact of stent-vessel (mal) apposition following carotid artery stenting: mind the gaps! Computer methods in biomechanics and biomedical engineering, 16(6):648–659, 2013.

Hai-Chao **Han**. Twisted blood vessels: symptoms, etiology and biomechanical mechanisms. Journal of vascular research, 49(3):185–197, 2012.

Konstantinos C **Koskinas**, Yiannis S Chatzizisis, Antonios P Antoniadis, and George D Giannoglou. Role of endothelial shear stress in stent restenosis and thrombosis: pathophysiologic mechanisms and implications for clinical translation. Journal of the American College of Cardiology, 59(15):1337–1349, 2012.

Dougal R **McClean** and Neal L Eigler. Stent design: implications for restenosis. Reviews in cardiovascular medicine, 3(S5):16–22, 2002.

Umberto **Morbiducci**, Annette M Kok, Brenda R Kwak, Peter H Stone, David A Steinman, Jolanda J Wentzel, et al. Atherosclerosis at arterial bifurcations: evidence for the role of haemodynamics and geometry. Thromb Haemost, 115(3):484–492, 2016.

P **Pancera**, M Ribul, B Presciuttini, and A Lechi. Prevalence of carotid artery kinking in 590 consecutive subjects evaluated by echocolordoppler. is there a correlation with arterial hypertension? Journal of internal medicine, 248(1):7–12, 2000.

REFERENCES

JFR **Paton**, CJ Dickinson, and G Mitchell. Harvey cushing and the regulation of blood pressure in giraffe, rat and man: introducing ”cushing’s mechanism”. Experimental physiology, 94(1):11–17, 2009.

Marina **Piccinelli**, Susanna Bacigaluppi, Edoardo Boccardi, Bogdan Ene-Iordache, Andrea Remuzzi, Alessandro Veneziani, and Luca Antiga. Geometry of the internal carotid artery and recurrent patterns in location, orientation, and rupture status of lateral aneurysms: an image-based computational study. Neurosurgery, 68(5):1270–1285, 2011.

Laura M **Sangalli**, Piercesare Secchi, Simone Vantini, and Alessandro Veneziani. Efficient estimation of three-dimensional curves and their derivatives by free-knot regression splines, applied to the analysis of inner carotid artery centrelines. Journal of the Royal Statistical Society: Series C (Applied Statistics), 58(3):285–306, 2009.

Dinko **Susic**. Hypertension, aging, and atherosclerosis: the endothelial interface. Medical clinics of north America, 81(5):1231–1240, 1997.

Esther AH **Warnert**, Jonathan CL Rodrigues, Amy E Burchell, Sandra Neumann, Laura EK Ratcli↵e, Nathan E Manghat, Ashley D Harris, Zoe Adams, Angus K Nightingale, Richard G Wise, et al. Is high blood pressure self-protection for the brain? Circulation research, 119(12):e140–e151, 2016.

Shanggang **Zhou** and Xiaotong Shen. Spatially adaptive regression splines and accurate knot selection schemes. Journal of the American Statistical Association, 96(453):247–259, 2001.

COMPMECH
Computational Mechanics & Advanced Materials

UNIVERSITÀ DI PAVIA

Thank you
for
your kind attention